FEATURE ARTICLE

Aromatic van der Waals Clusters: Structure and Nonrigidity

S. Sun and E. R. Bernstein*

Department of Chemistry, Colorado State University, Fort Collins, Colorado 80523-1872

Received: March 11, 1996; In Final Form: June 3, 1996[⊗]

More than a dozen cases of nonrigid van der Waals clusters are presented and discussed to demonstrate that cluster nonrigidity is a general phenomenon in all weakly bound systems. The interplay of structure and nonrigidity complicates cluster research and mandates a dynamical approach to cluster properties in which multiple stable configurations coexist and interconvert, and large amplitude nuclear motions are the rule rather than the exception. Empirical potential energy surface calculations are employed to yield physical insight into the structure and dynamics of nonrigid clusters, and molecular symmetry group theory is applied to analyze spectroscopic manifestations of cluster nonrigidity. Empirical potentials of various forms are successful in predicting most cluster structures, as well as estimating the potential surface barrier heights hindering the interconversion between different local minimum-energy structures. Such calculational approaches also emphasize the importance of large amplitude motion for one or more of the cluster vibrational degrees of freedom. The limits of these empirical calculations are discussed, and recent attempts to derive cluster structure and properties by ab initio techniques are reviewed. The aromatic/small molecule clusters considered in this presentation display two types of nonrigidity: local nonrigidity in which large amplitude motion involves the rotation of one of the molecular constituents, and global nonrigidity in which large amplitude motion involves displacement of the centers of mass of the molecular constituents. The former motion interchanges equivalent atoms, and the latter motion interchanges cluster conformations. The potential surface barriers for these large amplitude motions tend to increase with constituent molecule complexity.

I. Introduction

Structure determination is the primary and probably the most important step in the elucidation of molecular cluster properties. Only with a clear cluster structure in hand can one further pursue the study of the cluster potential energy surface and energy distribution processes for the cluster and, ultimately, elucidate chemical reactions that occur in clusters. Structure determination for a weakly bound van der Waals cluster is by no means a trivial step, and to date, only a few simple clusters have had their structures completely and unambiguously defined. The task of structure determination for van der Waals clusters is made especially difficult due to the complications of both large amplitude motion and cluster nonrigidity. In this context, cluster nonrigidity and large amplitude motion are related but not necessarily synonymous concepts. Cluster nonrigidity is defined as occurring for a cluster system in a given electronic state that has more than one energetically accessible potential minimum on its electronic potential energy surface. Large amplitude motion for intermolecular cluster modes (e.g., ±0.5 Å at the cluster mode zero point level) can involve only one, albeit flat, potential minimum. Nonetheless, large amplitude motion plays an essential role in the dynamical processes that connect different potential minima on a potential energy surface.

In the absence of a definite rigid cluster structure many conventional analysis techniques are no longer valid: such simplifying regimes include the Born−Oppenheimer approximation, the normal coordinate approximation, point group theory, and the assumption of a unique and well-defined cluster equilibrium structure. The entire notion of a nonrigid cluster presents challenges for cluster studies both experimentally and theoretically. The energy levels of a nonrigid cluster are quite different from, and more numerous at low energy than, those of a rigid system. Theoretically, nonrigidity also poses new challenges due to the more complex group theoretical classification of energy levels and more involved semiempirical and ab initio calculational algorithms required to reproduce the observed cluster potential energy surface. The absence of a rigid cluster structure requires that we view cluster geometry, dynamics, and reactivity from a new perspective.

Both molecules[1−4] and clusters[5,6] can be nonrigid, and in both instances, the origin of the nonrigidity lies in the multiminima nature of the potential energy surface for that particular electronic state: as the barriers between minima on a potential surface become small or zero, proper eigenfunctions of the system no longer correspond to solutions for the local minima. As a result, the system cannot be simply confined to a single potential minimum, and the system thereby loses its rigidity. Within a finite and detectable time scale the system can contort from one minimum energy conformation to another. Such large amplitude motion causes the observable energy levels to split or shift. By observing transitions between these split and shifted energy levels and comparing them to theoretical model predictions, one can uncover the nonrigid nature of the system under study. The lack of a rigid structure in these instances depends on the potential energy surfaces, the zero point energy, and the vibrational energy of the system. Ammonia is a frequently quoted example of a nonrigid molecule as the pyramidal skeleton has two equilibrium conformations between which it can tunnel due to inversion about its center of mass.[7] Another example of such a system is toluene, as the methyl group attached to the

---

Feature Article

J. Phys. Chem., Vol. 100, No. 32, 1996 **13349**

benzene ring can rotate nearly freely about the C−C single bond. Since toluene has a zero point vibrational energy in this "mode" of about 5 cm^{-1} and a barrier to rotation of about 10 cm^{-1}, we can say that it does not have a rigid equilibrium structure.[1,2]

Due to the weak van der Waals interactions between the molecules in a cluster, the potential barriers between the various equivalent and inequivalent equilibrium conformations of a cluster can be quite small. Therefore, nonrigidity is almost a universal phenomenon for clusters,[5,6] especially those containing only small molecules.[8] One of the early indications that aromatic/small molecule clusters are nonrigid can be found in the study of aniline/methane clusters.[9] The aniline $(CH_4)_1$ cluster origin consists of three unresolved peaks which form a broad feature with a full width at half-maximum of ca. 8 cm^{-1}. This is the first indication of a nonrigid cluster in which methane acts as an internal rotor above the plane of an aromatic molecule. Spectroscopic features due to internal motion in van der Waals clusters have now been classified for a number of systems with different limiting potential forms (hydrogen bonding, dispersion, etc.) and different species.[5] These studies now include experimental observations, theoretical treatments, and potential energy calculation results.

In this discussion, we present results for nonrigid aromatic/small molecule clusters and focus particular attention on examples that we have studied. New calculations are presented, as well, that describe the large amplitude modes in which the clusters are nonrigid. Following brief introductions to the experimental methods and the theoretical approaches for the study of cluster nonrigidity, we analyze more than a dozen nonrigid clusters in detail (e.g., benzene dimer, benzene/N_2, CO, CO_2, CH_4, NH_3, H_2O, toluene/N_2, H_2O, NH_3, CH_4).

II. Experimental Approaches

The basic technique for almost any spectroscopic study of weakly bound van der Waals clusters is the supersonic expansion because only under conditions of extreme cooling (temperatures ca. 50 K or below for the various degrees of freedom) will the clusters be stable and generate well-resolved spectra. With the exception of a few low-temperature matrix isolation experiments,[10] almost all studies of cluster nonrigidity are carried out in a supersonic beam.

Basically any spectroscopic method that can be employed to study clusters can be applied to extract information on the nature of cluster structure.

NMR spectroscopy is often used to determine structure and dynamical behavior in condensed phases;[11] however, since most nonrigid clusters are generated in a supersonic expansion with low concentrations of clusters, reports of NMR studies of nonrigid clusters are not available. With the ingenious application of pulsed Fourier transform (FT) techniques,[12] FT microwave spectroscopy has been successfully employed to study cluster structure and dynamics in a supersonic expansion environment. Rotationally resolved microwave spectra can be directly used to determine cluster structure and nonrigidity. For example, the benzene $(H_2O)_1$ cluster is determined to be a symmetric top,[13] which implies that the water molecule undergoes some degree of rapid motion above the benzene plane. The vibrationally averaged cluster structure must preserve a cluster axis of 3-fold or higher symmetry. The internal rotational energy levels of the water molecule can be derived from the spectrum.

Vibrational spectroscopy is an important component of the study of clusters, in general, as intermolecular modes give a direct access to the van der Waals potential. Infrared absorption can be measured employing a planar supersonic slit nozzle.[14]

An alternative approach to probing cluster vibrations for the ground electronic state is dispersed emission (DE) spectroscopy. In this technique emission from a particular vibronic level of the cluster is dispersed in a monochromator. Both inter- and intramolecular ground state modes can be detected in this manner. In many instances, this technique can be combined with mass-resolved excitation spectroscopy (MRES) to identify the cluster mass. Stimulated emission pumping (SEP) spectroscopy, employing two lasers to pump species into an excited electronic state and then dump them back to a ground state vibrational level, generates the same information as DE but at much higher resolution.[15]

Recently, two new techniques have been introduced for the probing of cluster ground state vibrations: ion-detected stimulated Raman spectroscopy (IDSRS)[16] and resonance ion-dip IR spectroscopy (RIDIRS).[17] Felker's group has performed IDSRS on a variety of clusters, mostly containing benzene. Through stimulated Raman transitions induced by two lasers, clusters in their ground electronic and vibrational state are excited to a Raman accessible ground state mode. A third laser probes the ground vibrational levels through a resonant multiphoton ionization in order to determine an ion gain (IGSRS) or an ion loss (ILSRS) signal. The two main advantages of this technique are mass selectivity and access to almost all vibrational levels of the ground electronic state cluster.[18]

RIDIRS is a similar and complementary technique to IDSRS and was first introduced by Lee and Shen.[19] It was later successfully applied by Zwier's group to the benzene/water cluster system to probe ground state vibrations and analyze cluster nonrigid behavior.[20] The RIDIRS technique is implemented as follows: ground electronic state vibrationless clusters are excited by direct laser absorption to an infrared accessible level, e.g., a CH or OH mode at ca. 3000 cm^{-1}, while another laser probes the cluster population of the vibrationless ground state through a mass selective ionization process. The ion dip signal, caused by IR absorption from the vibrationless level, reveals the ground state vibrational energies. Both IDSRS and RIDIRS are useful and important techniques in the study of nonrigid clusters because they are mass selective.

Ground state inter- and intramolecular vibrational data are vital to cluster research; they assist us in evaluating the cluster's potential energy surface and thereby local energy minima and their barriers. In some clusters, transitions between different contortional levels can be observed directly.

Clusters can also be probed on their excited electronic state surfaces by a similar array of fluorescence and mass selective techniques which access rovibronic states of the cluster. By monitoring either fluorescence or ion signals, excited state detection techniques are more sensitive than direct absorption and Raman measurements. The cluster potential energy surface of an excited electronic state often varies from that of the ground state; thus, different nonrigid behavior arises from different potential barriers and equilibrium geometries. Franck−Condon progressions in contortional coordinates found in excitation spectra often reveal nonrigid nature in both ground and excited states. Most typically, vibronic bands are well-resolved, and even rotational contours can be evaluated; in some instances, rotationally resolved cluster spectra can be obtained through fluorescence excitation (FE) spectroscopy and mass-resolved excitation spectroscopy (MRES).[21]

The experimental approach to the study of clusters in general, and nonrigid clusters in particular, that we have taken over the past 10 years has been vibronic state spectroscopy involving FE, DE, MRES, SEP, and hole burning.[1,5] In mass-resolved spectroscopy, an intemediate vibronic state of the cluster is

excited (typically $S_1 \leftarrow S_0$), from which a second photon ionizes the cluster ($I \leftarrow S_1$) near threshold to avoid cluster fragmentation and loss of mass identification. By scanning the excitation laser with the ionization laser fixed in frequency, the vibronic structure of the S_1 state can be determined as a function of the scanned laser wavelength and for a particular mass value of the clusters.

From these data we know the spectra of clusters of a fixed mass; however, clusters can have different structures for the same mass, as we shall see below, and we call these species isomers of a cluster of given mass value. For example, C_6H_6-$(Ar)_2$ can have two argon atoms on the same or different sides of the benzene ring. A cluster with more than one low-energy structure has multiple potential minima, and unlike a nonrigid cluster, the barriers on the potential surface to interconversion between the various isomeric structural forms are quite large. The difference between rigid cluster isomers and nonrigid clusters is conceptually small and operationally a function of the barrier height along interconversion paths. Interconversion between cluster isomeric forms, or cluster nonrigidity, is, of course, a function of cluster temperature. Typical cluster vibrational temperatures are on the order of 10 K, and thus many clusters with even 50 cm^{-1} barriers between isomeric forms can be considered rigid unless vibrationally excited.

Hole-burning (HB) spectroscopy can be employed to distinguish between isomers of clusters of a given mass. Since the first report of this technique in conjunction with supersonic jet spectroscopy,[22] it has been extensively employed for many systems to confirm cluster isomer spectral assignment.[23] Hole-burning spectroscopy consists of one probe laser fixed on a specific cluster vibronic transition while another (pump) laser scans through the wavelength region covering the cluster vibronic absorptions. The pump laser precedes the probe laser in time. A dip occurs in the probe laser generated signal (ion or fluorescence) if the pump- and probe-induced transitions share a common ground state energy level. Scanning of the pump laser over the region of the cluster isomer spectra will trace out the spectrum of a single isomer of the chosen mass (i.e., aromatic $(X)_n$). On the other hand, if the pump and probe lasers excite transitions on different cluster conformers, no HB spectrum will be observed. HB spectroscopy is thus both mass and structure selective. In some instance, HB spectroscopy also induces transitions involving large amplitude motion energy levels, thus directly revealing cluster nonrigidity.[5d]

In a broad sense, HB, IDSRS, and RIDIRS are related techniques because they all use a pump beam or beams to induce a transition in a species that is then detected by the forced change in a signal generated by a probe laser. The differences between these three approaches rest in the nature of the pump source and energy levels employed in the pump process: HB employs absorption to drive a vibronic transition, IDSRS employs stimulated Raman pumping to drive a ground electronic state Raman-allowed vibrational transition, and RIDIRS employs direct absorption to drive a ground electronic state infrared-allowed vibrational transition. Information gained from these studies on vibrational and vibronic states of clusters is, of course, complementary.

Employing many of the experimental methods introduced above, a number of nonrigid clusters have been investigated and characterized over the past 10−15 years. The aromatic chromophore species for many of these clusters include benzene, substituted benzenes, azabenzenes, and radicals such as benzyl ($C_6H_5CH_2$), cyclopentadienyl (C_5H_5, cpd), and substituted benzyls ($C_5H_4NCH_2$, etc.). Solvent or small coordination partners to these aromatic species include polar and nonpolar species from rare gases and diatomics to additional aromatics.

III. Theoretical Approaches

Spectroscopic results for nonrigid clusters are much more complex in general than for rigid clusters, and in order to analyze and interpret these data, theoretical models leading to potential energy surfaces for the motion of interest are essential. A good potential energy surface for a cluster should be able to reproduce binding energies for various conformations, intermolecular vibrations, barriers to conformational interconversion, and Franck−Condon factors for vibronic transitions. Approaches to these calculations vary from use of empirical atom−atom potential energy forms (e.g., Lennard-Jones−Coulomb, exponential-six, etc., see below) to rather extensive ab initio approaches. Detailed reviews of this general area can be found in refs 24 and 25.

Most ab initio calculations treat a cluster as a supermolecular system whose intermolecular energy is obtained by subtraction of the individual component molecular energies. The virtue of this approach is its conceptual simplicity, but its major drawback is the basis set superposition error (BSSE). The BSSE arises because the orbitals of the neighboring molecules will lower the energy of the subject molecule even in the absence of cluster formation. The energy reduction occurs simply because a larger basis set will always reduce the energy of a system. Corrections for the problem are made by expanding the molecular basis set until the energy is stable or by the counterpoise method of Boys and Bernardi.[26] This later technique calculates the energy of each molecular species in the full cluster basis set of all the molecules and uses this expanded basis set energy to compare the isolated molecule and cluster energy. The use of ab initio techniques has recently been expanding with the advent of better computers and programs. Ab initio calculation of cluster properties has been reviewed recently by Hobza et al.[27]

Theoretical calculations are an integral part of the cluster studies carried out in our laboratory. The approach we have adopted to these calculations is the application of empirical atom−atom potential energy functions. An entire cluster potential energy surface and the intermolecular vibrations can be calculated to a reasonable approximation in this manner. This approach is simple and economic, yet yields qualitatively correct, and in many instances, quantitatively accurate results.

Empirical potential energy calculations are based on a theoretically sound functional form and a set of universal atom−atom interaction parameters extracted from thermodynamic and crystal structure data. The potential forms and parameters are applicable to a wide range of systems from biological molecules to van der Waals clusters. Empirical potential energy calculations help generate physical insight into the binding energy and structure of clusters, the barriers to internal motion, and the nature of the interactions that are important for cluster behavior. Such calculations can serve to predict cluster properties and guide cluster experimental studies.

In a cluster empirical potential energy calculation, each molecule is treated initially as a rigid body which does not deform during the cluster formation. The cluster interaction is decomposed into the sum of atomic pairwise interactions between the atoms of the different molecular constituents of the cluster. For atom−atom pairwise interactions, short-range repulsion, induction and dispersion interactions, and electrostatic interactions are expressed in different forms. Short-range repulsion and the induction/dispersion interactions can be simulated in several different ways: two of them used by our group to calculate cluster interactions are Lennard-Jones (L-

Feature Article

J. Phys. Chem., Vol. 100, No. 32, 1996 **13351**

J)[28] and the exponential-six (exp-6)[29] potential forms. In the most frequently quoted L-J potential form, repulsive and attractive interactions between a pair of atoms are modeled by A_{ij}/r_{ij}^{12} and $-C_{ij}/r_{ij}^{6}$, respectively, while for exp-6 form, they are represented as $A'_{ij} \exp(-B'_{ij} r_{ij})$ and $-C'_{ij}/r_{ij}^{6}$, respectively. Here r_{ij} is the distance between the atoms i and j, and A_{ij}, C_{ij}, A'_{ij}, B'_{ij}, and C'_{ij} are empirical coefficients derived from a universal set of atom−atom interaction parameters. They are, of course, specific for each set of interacting atoms.[30] The electrostatic interaction term is treated as the sum of the Coulomb interactions, $q_i q_j/D r_{ij}$, between the pair of atoms with partial charges q_i and q_j. The constant D in this expression is the dielectric constant. Even though the interaction occurs in a vacuum for which $D = 1$, the potential parameters are derived from condensed phase data, and $D = 2$ is often used empirically in many calculations.[30] A hydrogen bond is simulated specifically by a separate potential form: $A_{ij}^{hb}/r_{ij}^{12} - C_{ij}^{hb}/r_{ij}^{10}$. Therefore, the total cluster interaction is expressed (using L-J potential) in the (6−12−1−10−12) form as

$$E = \sum_{i=1}^{n} \sum_{j=1}^{m} \{(A_{ij}/r_{ij}^{12} - C_{ij}/r_{ij}^{6})(1 - \delta_{ij}^{hb}) + q_i q_j/D r_{ij} + (A_{ij}^{hb}/r_{ij}^{12} - C_{ij}^{hb}/r_{ij}^{10})\delta_{ij}^{hb}\} \quad (1)$$

The delta function δ_{ij}^{hb} is 1 if the atoms i and j can undergo hydrogen bonding (e.g., $i =$ H, $j =$ O, N, S, ...), and δ_{ij}^{hb} is 0 otherwise. This device simply adjusts the potential form for the appropriate atom types.

With eq 1 the cluster potential energy surface (PES) is completely mapped out, and the binding energy is the potential minimum at the equilibrium geometry. To compare calculated and experimental results and make assignments or predictions of vibrational bands, a normal coordinate analysis (NCA) can be applied to the van der Waals cluster by employing the FG matrix method of Wilson et al.[31] Treating the whole cluster as a "giant molecule" with total N atoms, $3N - 6$ harmonic oscillator equations are solved for their eigenvectors and eigenvalues.[32] Assuming that the intramolecular vibrations are uncoupled from the low-frequency intermolecular modes, we are able to distinguish all the intermolecular vibrations and their eigenvectors from the total $3N - 6$ modes. This NCA method yields clear physical pictures of the intermolecular vibrations and has been applied to make assignments of transitions to particular modes.

A major drawback to this approximation is that many intermolecular vibrations are extremely anharmonic, especially for those modes in a nonrigid cluster for which the potential surfaces are flat or with very small barrier to large amplitude linear or cyclic motion. In such nonrigid clusters or for combinations and overtones an NCA is no longer valid. Miller et al.[33] have shown that the full potential energy functional form can be used in the Schrödinger equation which is solved numerically. This gives a much more accurate representation of the vibrational motion than does the harmonic oscillator approach. Nonetheless, with very flat potential surfaces or with surfaces that have very low barriers to internal translation and rotation, even this calculational method becomes problematic: large amplitude contortional motions arise which transform clusters from one potential minimum to another. The contortional mode in the system Hamiltonian must be separated and dealt with independently.[34] Generally, two types of contortional motions exist in a nonrigid cluster: large amplitude vibration in a flat-bottomed potential well and internal rotation in a cyclic potential.

The first type is often observed when the solvent molecule has two or more symmetrical equilibrium minima along a translational coordinate, while the potential barriers between the minima are quite shallow at least in one degree of freedom. This type of potential (W-shape) can be modeled by one of two forms:

$$V(Q) = \tfrac{1}{2}aQ^2 + b \exp(-cQ^2) \quad (2)$$

with potential barrier b, or

$$V(Q) = AQ^2 + BQ^4 \quad (3)$$

with potential barrier $A^2/4B$.[2a] The significant quadratic term in these flat-bottomed wells destroys the harmonicity of the vibrations.

The second type of contortional motion, internal rotation, appears more frequently in large nonrigid clusters. For the simple one-dimensional model of the internal rotor with n-fold symmetry, the Hamiltonian is[1,2b]

$$\hat{H} = -B\frac{\partial^2}{\partial \phi^2} + V(\phi) \quad (4)$$

in which B is the effective or reduced rotational constant associated with the internal rotation, and the cyclic potential barrier is represented as

$$V(\phi) = \tfrac{1}{2}\sum_{k=1}^{\infty} V_k[1 - \cos(nk\phi)] \quad (5)$$

In practice, only the first one or two V_k terms are required to model the energy levels observed, and the Schrödinger equation can be solved within a basis set of free rotor wave functions ($e^{im\phi}$, $m = 0, \pm 1, \pm 2, ...$). Besides the one-dimensional model of the internal rotor, two-dimensional[20] and three-dimensional[35] rotor models have also been reported. The physical and mathematical principles of these models are the same, and usually the one-dimensional hindered rotor model is adequate to assign most experimental spectra.

Another important aspect of nonrigid cluster study is the new group theory approach required. Due to the absence of a rigid cluster equilibrium configuration, point group symmetry analysis is invalid for nonrigid clusters. Molecular symmetry (MS) group analysis, which is based on the permutation−inversion (PI) group theory developed in the 1960s,[36] can account for nonrigid structure and contortional motions. With the optical selection rules developed in the MS group, one can determine the allowed and forbidden transitions between the various contortional levels of a nonrigid cluster. The details of the MS group analysis will be briefly covered for particular case studies of interest below. We should point out, nonetheless, that the MS group also has its limitations: practically it can only deal with small systems of limited contortional motion at present. Even a system as small as the benzene dimer, if a number of internal motions become accessible (low barrier to interconversion between structural isomers), the size of the groups involved become completely unwieldy (i.e., the number of group elements becomes much greater than 10^3).

IV. Individual Case Studies

A. Benzene/N$_2$, CO, CO$_2$. The simplest clusters containing the prototypic aromatic molecule benzene are, of course, the clusters formed from benzene and the rare gases. The next level in complexity for benzene clusters is benzene/diatomic molecule
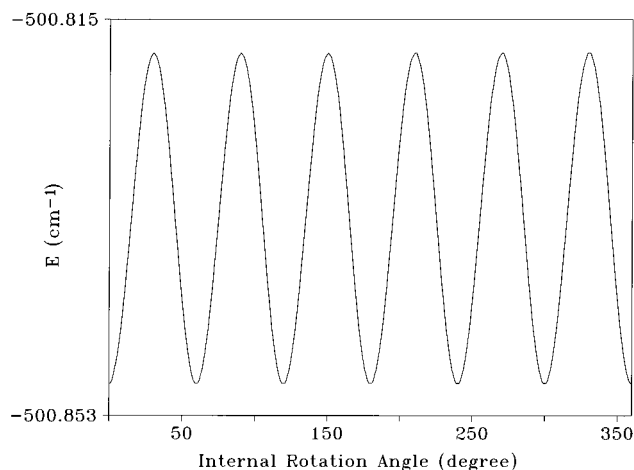
Figure 1. Calculated 6-fold potential barrier for the internal rotation of benzene$(N_2)_1$ cluster. The solvent molecule N_2 is rotating about the axis passing through its center of mass and perpendicular to the aromatic plane. The barrier height here is about 0.03 cm^{-1}.

TABLE 1: Calculated Results of Benzene/X Clusters, Based on L-J−Coulomb Potential

cluster	intermolecular distance^a R (Å)	binding energy E_b (cm^{-1})	S_z van der Waals stretch^b ν_z (cm^{-1})	internal rotor barrier E_{rot} (cm^{-1})
benzene$(N_2)_1$	3.31	501	62	0.031
benzene$(CO)_1$	3.24	622	68	0.084
benzene$(CO_2)_1$	3.27	861	71	1.016

^{a} R is the distance between the centers of mass of the two molecules. ^{b} ν_z is the out-of-plane symmetric stretch mode.

species, and even for this system, nonrigid cluster behavior occurs and can be characterized. Benzene/N_2, CO, CO_2 clusters have been studied by two-color threshold ionization MRES.[5a,6,37−39] Since CO_2 is a linear nonpolar triatomic, its behavior in a benzene cluster is quite similar to that found for N_2 and CO.

Through L-J empirical potential energy calculations, both N_2 and CO_2 are found to coordinate to the π-system of the benzene ring with their centers of mass coinciding with the 6-fold benzene axis and their bond axes perpendicular to this axis. The benzene$(CO)_1$ cluster configuration is somewhat different; the CO bond axis is found to be tilted by $\sim$15° from the horizontal ring plane with its O atom closer to the benzene ring plane. This tilt can be associated with the small dipole moment of CO ($\sim$0.12 D); if the partial charges on CO increase appropriately, the tilt angle also increases. The projection of the three solvent molecules onto the ring plane bisects the benzene C−C bonds. Rotating the N_2, CO, and CO_2 molecules around the benzene 6-fold axis generates six symmetrical minimum-energy geometries with small potential barriers ($\leq$1 cm^{-1}) between them. Figure 1 presents an example of such a 6-fold potential barrier for the benzene$(N_2)_1$ cluster. Table 1 lists the calculated solute−solvent intermolecular distances, binding energies, and out-of-plane (Z-axis) van der Waals stretch energies, as well as the potential barriers to internal rotation for these three systems.

On the other hand, solvent molecule rotation about an axis parallel to the benzene ring and perpendicular to the linear molecule bond axis is impossible. As an example, Figure 2 shows the calculated potential barrier ($\sim$540 cm^{-1}) for N_2 rotation about an axis parallel to the ring and perpendicular to the N−N bond. Thus, the internal rotation in the cluster is only one-dimensional, and the other degree of rotational freedom is vibrational in nature.
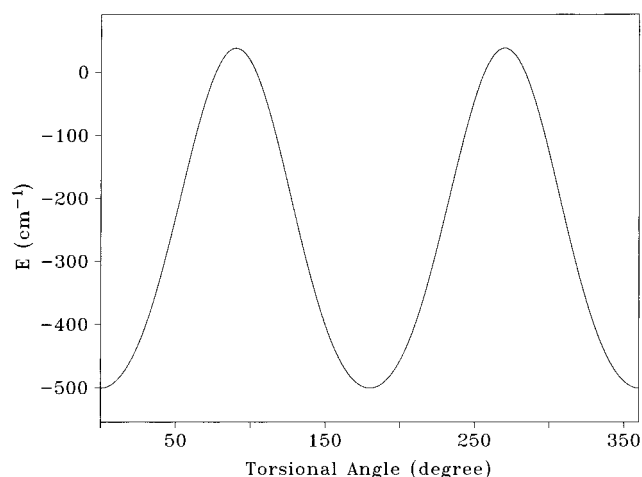

Figure 2. Calculated 2-fold potential barrier for the benzene$(N_2)_1$ cluster torsional motion, in which N_2 is rotating about the axis passing through its center of mass and parallel to the aromatic plane. The barrier height here is more than 500 cm^{-1}.
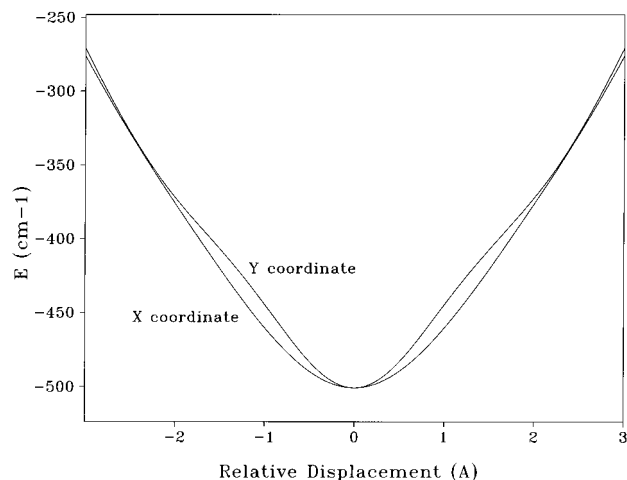

Figure 3. Calculated potential surfaces for the bending modes (b_x and b_y) of benzene$(N_2)_1$ cluster. Notice the relatively flat, anharmonic potential well at the bottom.

Translational motions of the solvent molecule relative to benzene result in three intermolecular vibrations: one out-of-plane stretching mode (Table 1) and two in-plane bending modes. Figure 3 depicts the calculated potential curve for these bending coordinates in the benzene$(N_2)_1$ cluster. We can see that, even at the zero-point energy level ($\sim$10 cm^{-1}), the N_2 is able to move from the benzene 6-fold axis by ca. $\pm$0.5 Å. Due to this flat potential surface, the two van der Waals modes have very low vibrational energies. This surface suggests that such motion is poorly approximated by a harmonic oscillator model. The significance of those large amplitude motions will be discussed later.

Additionally, rotationally resolved spectra have been obtained for benzene$(N_2)_1$ and $(CO)_1$ van der Waals clusters.[6,37] Weber et al. obtain a rotationally resolved spectrum for the 6_0^1 benzene$(N_2)_1$ vibronic transition, from which they derived the rotational constants for both the ground and excited electronic states.[6a] Using $^{15}N_2$ to reduce spectral congestion, Ohshima et al. perform Fourier transform microwave spectroscopy on the benzene$(^{15}N_2)_1$ cluster and analyze the ground electronic state structure of the cluster.[6c] Brupbacher et al. also analyze the microwave spectrum of benzene$(CO)_1$ and fit it to the structure of a symmetric top.[37] All these rotationally resolved spectra of benzene/diatomic molecule clusters agree with the original conclusion, based on direct observation of vibronic transitions

Feature Article

J. Phys. Chem., Vol. 100, No. 32, 1996 **13353**

(at 0_0^0 and 6_0^1) involving internal rotational energy levels of the clusters, that the diatomic lies on top of the benzene ring and undergoes nearly unhindered internal rotation about the benzene C_6 molecular axis. The intermolecular distances between the molecular centers of mass of C_6H_6 and N_2 are given as 3.502 and 3.457 Å for S_0 and S_1 electronic states of the cluster,[6a] respectively. The microwave result for this ground electronic state distance yields 3.498 Å.[6c] For the benzene(CO)$_1$ cluster, the angle of CO incline to the plane of the benzene ring is ~4.6° (C atom closer to the ring), and its center-of-mass distance is 3.44 Å.[37] In all of these high-resolution studies the barriers to internal rotation are assumed to be very small.

Besides our empirical potential energy calculations, ab initio studies have been performed on the benzene(N$_2$)$_1$[6b] and the benzene(CO)[38] van der Waals clusters. Hobza et al.'s calculation[6b] on the ground state benzene(N$_2$)$_1$ reveals the same cluster structure as determined previously, with an intermolecular distance of 3.4 Å at the potential minimum, a binding energy of 591 cm^{-1} (520 cm^{-1} if considering the ZPE), and an out-of-plane van der Waals stretch frequency of 56.6 cm^{-1}. The N_2 molecule is able to rotate freely about the benzene C_6 axis. Calculations for benzene(CO) by Nagy et al. yield a similar picture.[38] The intermolecular distance between CO and benzene is 3.32 Å, and the out-of-plane van der Waals stretch frequency is 71 cm^{-1}. The CO molecule is tilted from the parallel-to-benzene position by ~5.2° with the O atom closer to the ring plane. The cluster binding energy is significantly underestimated, probably due to the small basis set employed for CO. Both calculations at the ab initio level are consistent with the simple empirical potential energy for clusters. The point best made here is that theory, in the form of either ab initio or empirical potential energy calculations, can be employed to describe the physically correct picture for simple van der Waals clusters. The one point of disagreement between theory and experiment for the benzene (CO)$_1$ system is which atom lies closest to the aromatic ring. While this is not a trivial point by any means, it is not terribly surprising in light of the subtle nature of the charge distribution and interaction for the CO molecule.

To understand the internal rotational behavior (energy levels and barriers) of these van der Waals clusters, the starting point is a normal coordinate analysis (harmonic oscillator approximation). This approach is applied to benzene/N$_2$ CO, CO$_2$ clusters and shows that the Z-axis rotation is inadequately treated and that the vibronic spectra of the cluster cannot be reasonably analyzed within this model. This degree of freedom is then treated as an internal rotation with the theory of the molecular symmetry group for nonrigid molecules. Using the MS group G_{24}^5 for benzene/N$_2$, CO$_2$ and G_{12}^3 for benzene/CO, we are able to fit and assign all the bands associated with internal rotational level transitions for the 0_0^0 and 6_0^1 transitions of the respective clusters.[5a] Larin et al.[39] recalculated these levels within a model employing a two-dimensional rotor and a spherical harmonic basis set. Their band assignments are essentially identical to the original ones,[5a] and their results indicate that the barriers to internal rotation are quite small for the parallel to benzene rotation (~1 cm^{-1}) and large for the other torsional modes.

Within the context of a normal coordinate/harmonic oscillator/ C_{2v} point group approximations for the benzene/N$_2$, CO$_2$ clusters, vibronic transitions to the bending mode fundamentals (b_x, b_y) are forbidden within the cluster 0_0^0 structure. Transitions most likely associated with these modes were originally assigned as overtones of the bends.[5a] Employing IDSRS, Venturo et al. observed a single Raman-active vibration of about 38 cm^{-1} for benzene(N$_2$)$_1$ and assigned it as the fundamental,
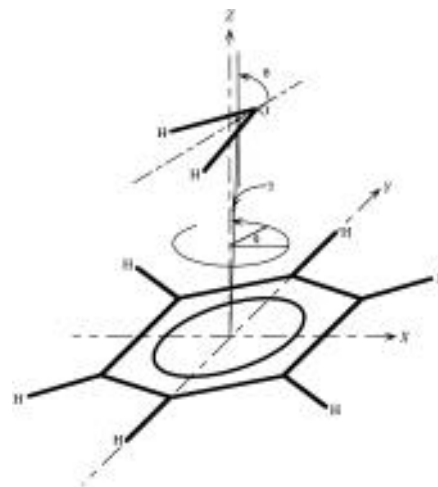

Figure 4. Diagram showing the calculated stable configuration of the Bz(H$_2$O)$_1$ cluster. The center of mass of H$_2$O is slightly off the C_6 axis of benzene by 0.24 Å, and the intermolecular distance is 3.16 Å. The two H atoms of H$_2$O are 0.21 Å closer to the benzene plane than the O atom. The internal rotation of H$_2$O around the C_6 axis of benzene (ϕ) has a 6-fold potential barrier of only ~0.05 cm^{-1}.

rather than the overtone, of a van der Waals bending mode.[18b] In a later paper[40] they pointed out that the large amplitude motions in these van der Waals modes can impart substantial intensity to the fundamental bands of the intermolecular bending modes.

In summary, benzene(N$_2$)$_1$, benzene(CO)$_1$, and benzene(CO$_2$)$_1$ clusters have been studied by vibronic, rotational, and vibrational spectroscopic methods. Theoretical calculations at both empirical and ab initio levels have also been carried out for these three simple clusters. All three linear solvent molecules can freely rotate about the benzene C_6 axis, and the van der Waals bending modes involve large amplitude motions. All the spectral features can be assigned in a MS group analysis.

B. Benzene/H$_2$O, NH$_3$, CH$_4$. The benzene/H$_2$O, NH$_3$, CH$_4$ clusters represent a higher level of complexity for benzene/X clusters than do the benzene/N$_2$, CO, CO$_2$ clusters. Understanding their spectra and structures is both of theoretical and practical significance. For example, the benzene(H$_2$O)$_1$ cluster is believed to have a weak hydrogen-bonding interaction between the water hydrogens and delocalized π-electrons of the aromatic ring. The benzene/X system is the simplest one in which to study interactions between an aromatic molecule and nonpolar, polar, and hydrogen-bonding solvents. Consequently, these clusters have been the subject of many studies. Clearly, biological systems could have similar interactions that would help stabilize and control macromolecule/solvent structure and properties.

The first MRES spectrum of the benzene/H$_2$O cluster system was obtained more than 10 year ago.[41] van der Waals features on the cluster 0_0^0 and 6_0^1 transitions were assigned based on empirical potential energy calculations and the tacit assumption of a rigid cluster structure. The calculated ground state cluster structure is given in Figure 4 at the potential energy minimum: the cluster has C_s point group symmetry with a distance between the molecular centers of mass of 3.16 Å. The H$_2$O center of mass is off the C_6 axis of benzene by 0.24 Å, which yields a small angle γ of ~4.4° between the benzene C_6 axis and the line passing through both molecular centers of mass. The water molecular plane is not parallel to the benzene molecular plane as the two hydrogen atoms of the water molecule are 0.21 Å closer to the benzene ring than is the oxygen atom of water. This structure suggests that a generalized hydrogen-bonding interaction occurs between the water molecule and the de-

TABLE 2: Experimental and Calculational Results for Intermolecular Distance, Binding Energy, Angle between C_2-C_6 Axes, and the Internal Rotor Barrier of Benzene$(H_2O_1)_1$ for a L-J—Coulomb Potential

study	R_{CM-CM} (Å)[a]	$E_{binding}$ (cm^{-1})	C_2C_6 axes angle θ^b (deg)	internal rotor barrier V_6 (cm^{-1})
Zwier et al.[c]	3.32	570−973	52	≤2
Augspurger et al.[50]	3.266	1303	53	1.6
Gutowsky et al.[13a]	3.329		37	∼0
Susuki et al.[13b] FTMW exp	3.347		20 ± 15	∼0
Suzuki et al.[13b] ab initio calc	3.195	≥623	24	0.17
our work	3.167	505	68	0.05

[a] Distance between centers of mass of benzene and H_2O. [b] Angle between C_2 axis of H_2O and C_6 axis of benzene. [c] Combined results from refs 20, 42, and 43.

localized π-electron distribution of the benzene molecule. The angle θ between the C_2 axis of water and the C_6 axis of benzene is ∼68°.

While not discussed in the original study,[41] this cluster has two internal degrees of freedom that are nonrigid: the internal rotation of the H_2O molecule about the C_6 axis of benzene, and the large amplitude libration that interchanges the two hydrogen atoms. Similar to the case of benzene$(N_2)_1$ discussed above, the internal rotation of H_2O about the benzene C_6 axis is practically unhindered (V_6 ∼0.05 cm^{-1}) in the ground electronic state. The exchange of two H_2O hydrogen atoms through a librational motion is somewhat more complex. Rotation of H_2O about its C_2 axis is unfeasible due to a barrier height of >750 cm^{-1}. The out-of-plane wagging mode of H_2O has a potential barrier of >160 cm^{-1} if the H_2O center of mass is held fixed; however, if the H_2O molecular center of mass is allowed to translate in the $+Z$ direction, the barrier to interchange of the two hydrogens by a combined wag and stretch is as low as 20 cm^{-1}. The H_2O torsional motion about an axis perpendicular to its C_2 axis and its molecular plane has a barrier of about 80 cm^{-1}. This well is quite flat for motion as large as ±50° (20 cm^{-1} gain in potential energy), and this motion is certainly of large amplitude. In general, motions of the water molecule which keep the atoms at nearly the same distance above the benzene plane are feasible, but ones that change these distances significantly are unfeasible (large barrier to the motion).

A number of other groups have studied the structure of benzene$(H_2O)_1$ clusters[13,17,42−45] and have tried to model its nonrigid behavior. Among them, Zwier's group has performed REMPI spectroscopy to obtain rotational band contours[42,43] and RIDIRS to probe the C−H and O−H stretch frequencies of the cluster.[17,20] Their model of the benzene$(H_2O)_1$ cluster is somewhat different from that described above and depicted in Figure 4. In their picture the plane of the water molecule is perpendicular to the benzene plane, the water center of mass is on the C_6 axis of benzene, and one of the H_2O O−H bond axes is perpendicular to the benzene ring. The in-plane torsional motion, which can interchange the two inequivalent water H atoms, has a very flat potential well, allowing large amplitude displacements of the H atoms (±52° in the zero-point level). Rotation of water about the C_6 axis has almost no barrier.

Despite the differences between these two models, many common factors arise in their physical description of the benzene$(H_2O)_1$ cluster. Both models require free internal rotation of water about the C_6 axis of benzene and thus predict a nearly symmetric top behavior for the overall cluster rotational states, and in-plane water torsional motion is of large amplitude (±50°).

Jönsson et al.[46] proposed a modified L-J potential form for the benzene/H_2O interaction. The calculated structure based on this potential form (1−4−6−9−12) is more like that of the Zwier model than of the earlier one.[32] This potential form generates a second cluster structure with water in the plane of

the benzene ring and no hydrogen bonding from water to the π-system. Since no experimental evidence for a second cluster structure has been presented, one must use this modified potential form with some care.

A number of groups have reported ab initio calculations for the benzene/H_2O clusters.[13b,46−50] At the highest level, the calculations predict inequivalent water molecule H atom positions and a large amplitude torsional motion.[13b,50a] Using a molecular mechanics on clusters (MMC) approach, a global minimum for the structure is found with the C_2 axis of water making a ∼50° angle with the C_6 axis of benzene.[50]

High-resolution, rotationally resolved spectroscopy has not been as helpful as one would like in resolving a "final" benzene$(H_2O)_1$ structure, partially due to the nonrigid nature of the cluster itself. Recall that every spectral analysis starts with a model structure, and if the one chosen is nonrigid, a unique structure is not forthcoming from the data analysis. Fourier transform microwave spectra for benzene$(H_2O)_1$ are reported by Suzuki et al.[13b] for high-J (≥4) and by Gutowsky et al.[13a] for low-J (0, 1, ..., 4) transitions. Both experimental interpretations support a symmetric top "structure", mandating the free internal rotation of the water molecule. The angle between the C_2 axis of H_2O and the C_6 axis of benzene is calculated to be around 37° by Gutowsky et al.[13a] and 24° by Suzuki et al.[13b] The present experimental data and analyses are insufficient to distinguish between the two models presented above. Table 2 summarizes the various cluster parameters obtained through both experiments and calculations.

In addition to the rotational motion of the H_2O molecule in the benzene$(H_2O)_1$ cluster, the translational motion of H_2O parallel to the benzene plane is also of large amplitude. Even at the zero-point energy of these "bending" modes, the H_2O molecule is calculated to be able to experience ±0.5 Å translational amplitude displacements from its equilibrium position. Felker's group performed IDSRS experiments on benzene/H_2O clusters and observed Raman-active bands in the energy range 5−10 cm^{-1} for benzene$(H_2O)_1$. They tentatively attributed these modes to low-frequency in-plane torsional vibrations. Features between 30 and 50 cm^{-1} are assigned to bending modes of the cluster.[45] The strong Raman activity of these modes again indicates that large amplitude motion and cluster nonrigidity are important for the benzene/H_2O cluster interactions and structure.

The situation, both experiment and theoretical, with regard to the "structure" of benzene$(H_2O)_1$, and indeed the entire benzene/H_2O cluster system, is still evolving. The benzene-$(H_2O)_1$ cluster is certainly nonrigid; a better structural description than "a symmetric top" (C_3 or higher point group symmetry) with a certain C_2 water axis/C_6 benzene axis angle at present does not seem to be readily accessible. One must now generate an appropriate molecular symmetry group for the cluster, taking into account the feasible and unfeasible nonrigid, contortional motion for the system so that spectroscopic transitions can be

Feature Article

J. Phys. Chem., Vol. 100, No. 32, 1996 **13355**

predicted and identified. This is, of course, a nontrivial task. Zwier et al.[43] have made considerable progress along these lines employing the G_{24} MS group.

Mass-resolved excitation spectra of the benzene$(CH_4)_1$ cluster in the benzene 6_0^1 region has been reported nearly 10 years ago.[51] No 0_0^0 spectrum is observed for this cluster, suggesting that the cluster structure has at least a 3-fold symmetry axis. Both exp-6 and L-J empirical potential energy calculations have been performed for this system, and they result in the same C_{3v} cluster equilibrium geometry, with one C–H bond on the C_6 axis of benzene and the other three C–H bonds point toward the benzene ring (i.e., three CH_4 H atoms close to the ring and one away from the ring with the C atom on the C_6 axis). The binding energies calculated by the two potentials are 599 (exp-6) and 540 cm^{-1} (L-J), and the cluster center-of-mass equilibrium distance is 3.42 and 3.47 Å, respectively, for the two potential forms. Similar experimental and theoretical studies are reported for benzene/CD_4 and CF_4 clusters.[35]

This latter reference reported incorrectly that all these clusters are rigid. The error of this work is to assume that CH_4 would rotate about its highest symmetry (S_4) axis instead of its unique (in the cluster) C–H bond, C_3 axis. We have recalculated the potential energy surface for this cluster with an L-J potential form: CH_4 rotation about the cluster C_3 axis has a V_6 hindering potential of 0.74 cm^{-1}. Thus, the cluster is nonrigid for Z-axis rotation of CH_4. The cluster is rigid for any rotation about an axis perpendicular to the C_3 axis (parallel to the ring plane). The interchange of the Z-axis H atom with the other three CH_4 H atoms is unfeasible.

Note, however, that apparently no transitions associated with this nonrigid motion are observed in the spectrum of this cluster. This is probably due to both Franck–Condon factors and the similarity of the ground and excited state potential surfaces.

The doubly degenerate bending mode (b_{xy}) of this cluster, which involves motion of the CH_4 molecule parallel to the benzene plane, is again calculated to be of large amplitude: within the zero-point level of this bending mode the CH_4 can translate ±0.5 Å over the benzene ring. This mode can have intensity in both Raman and vibronic spectra through two mechanisms: Herzberg–Teller vibronic coupling[5b] and/or large amplitude motion induced Herzberg–Teller coupling.[40]

Two ab initio calculations have been reported for the benzene-$(CH_4)_1$ cluster, and they each yield different structures. Using an MP2/6-31G*//HF/3-21G algorithm, Brédas and Street calculated two stable cluster structures:[48] a C_{3v} point group symmetry structure as discussed above (binding energy = 357 cm^{-1} and center-of-mass distance between the two molecules $= R_{CM–CM} = 3.71$ Å) and a C_{2v} point group symmetry structure with the CH_4 above the benzene ring (binding energy = 423 cm^{-1} and center-of-mass distance = 3.75 Å). This calculation gives the low-symmetry cluster as the more stable one. While this calculation gives the cluster binding energy too low (the cluster does not dissociate with 6_0^1 excitation) and spectroscopic evidence is inconsistent with two cluster geometries and any geometry with C_{2v} symmetry (no 0_0^0 feature observed), it does demonstrate a flat potential near these equilibrium positions and thus large amplitude motion for ready interconversion between these two cluster structures. The Brédes and Street calculation suggests that the benzene$(CH_4)_1$ cluster should be nonrigid. Sakaki et al. performed ab initio SCF/MP2-MP4 calculations of eight different conformations of benzene/CH_4 molecules.[52] The binding energy for the cluster is 682 cm^{-1} ($R_{CM–CM} = 4.07$ Å) from MP2/MIDI-4** calculations and 381 cm^{-1} ($R_{CM–CM} = 3.82$ Å) from MP2/6-31G** calculations. Both procedures yield the same C_{3v} symmetry structure with one

hydrogen pointing toward the benzene ring and three pointing away from it. No discussion of benzene$(CH_4)_1$ nonrigidity is presented in this work. At present, ab initio calculations do not offer a better insight into the cluster structure and behavior than do empirical potential energy calculations.

No molecular symmetry (MS) group analysis has been conducted for the benzene$(CH_4)_1$ cluster. The free CH_4 molecule has 24 feasible operations which form the T_d (MS) group.[34] If all permutation operations for hydrogen atoms of CH_4 were feasible within the benzene$(CH_4)_1$ cluster, the molecular symmetry group would have 144 feasible operations to form a G_{144} MS group. If only the three equivalent hydrogens could exchange, the MS group would reduce to G_{36}. Applying this G_{36} group to the cluster would generate selection rules for transitions between the different contortional levels of the CH_4 one-dimensional rotor. To assign the various spectra of this cluster completely, one would need such an MS group analysis.

MRES for benzene$(NH_3)_1$ were presented by Wanna et al. for the cluster 0_0^0 and 6_0^1 regions.[41] These vibronic spectra are quite congested, but since the 0_0^0 of the cluster is observed, at least one cluster structure has no 3-fold axis. L-J empirical potential energy calculations yield two stable cluster structures for the benzene$(NH_3)_1$ cluster: one has a C_{3v} symmetry with apparent hydrogen bonding between the NH_3 H atoms and the benzene ring π-system (like benzene$(CH_4)_1$ with the lone pair of N electrons occupying the distant H position), and the other has a C_s symmetry with two N–H bonds of NH_3 at an angle of ca. 47° to the benzene ring plane and the third at an angle of ca. 73° to the ring plane on the C_s plane of the complex. Figure 5 depicts these two structures. The binding energy of the C_{3v} cluster is 711 cm^{-1}, and $R_{CM–CM} = 3.24$ Å. Rotating NH_3 about the principal axis of the C_{3v} cluster (Z) generates a 6-fold potential barrier $V_6 \sim 1.1$ cm^{-1}. Thus, the C_{3v} benzene$(NH_3)_1$ cluster has a nearly freely rotating NH_3 group lying above the plane of the benzene ring, hydrogen bonded to the ring π-system. Vibronic transitions for this cluster configuration can only be observed in the 6_0^1 region of the spectrum, not the 0_0^0 region, because of electronic state selection rules. The doubly degenerate bending mode (b_{xy}) of this cluster configuration is also a large amplitude motion. According to these potential energy calculations, the NH_3 molecule can move ±0.4 Å in its zero-point level over the plane of the benzene ring.

The center of mass of NH_3 for the C_s benzene$(NH_3)_1$ cluster is 0.2 Å off the C_6 axis of the benzene ring with its 3-fold axis about +5° out of a plane parallel to the ring plane. The binding energy for the C_s configuration is calculated to be 608 cm^{-1} with $R_{CM–CM} = 3.32$ Å. Rotating the NH_3 about the C_6 axis of benzene generates a potential barrier V_6 of ca. 0.2 cm^{-1}: again, we find free rotation in this cluster system. Rotation of the NH_3 about its 3-fold axis has a potential barrier of ca. 250 cm^{-1}, and thus the NH_3 H atoms cannot exchange. The bending motion, NH_3 translation parallel to the ring plane, is also of large amplitude, and the zero-point level displacement is roughly ±0.4 Å.

Investigation of the potential energy surface separating these two benzene/NH_3 cluster configurations proves to be quite interesting. Since the benzene–NH_3 intermolecular center-of-mass difference for the two configurations is so small, we first explore the rotational coordinate for NH_3 about an axis parallel to the ring plane. Figure 6 shows the potential curve as a function of the rotation angle ϕ (see Figure 5). This rotation axis passes through the center of mass of the NH_3 molecule and is perpendicular to both the C_3 axis of NH_3 and the C_6 axis of benzene. $\phi = 0°$ corresponds to the C_s configuration, and $\phi = +95°$ corresponds to the C_{3v} configuration. At $\phi = +95°$
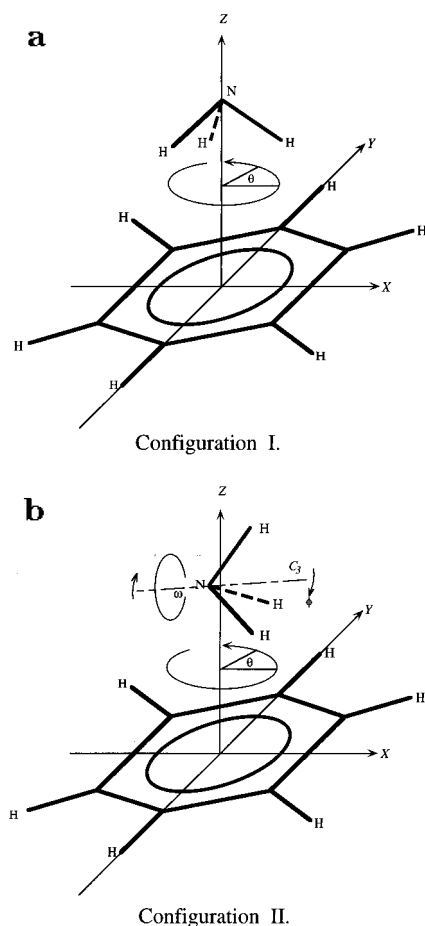
a

Configuration I.

b

Configuration II.

Figure 5. Diagram showing the two calculated stable configurations of the Bz(NH$_3$)$_1$ cluster. Configuration **I** has an apparent C_{3v} geometry, though the internal rotation of NH$_3$ about the Z axis has a potential barrier of only 1.1 cm^{-1}. In configuration **II** (C_s), the C_3 symmetry axis of NH$_3$ is 5° out of a plane parallel to the benzene ring, and the center of mass of NH$_3$ is 0.2 Å off the C_6 axis of benzene. The intermolecular distances of these two configurations are 3.24 and 3.32 Å, respectively.
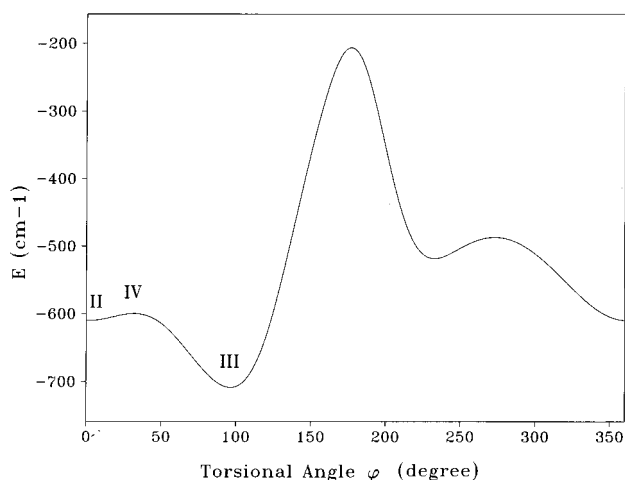

Figure 6. Calculated potential surface for the internal torsional rotation of the benzene(NH$_3$)$_1$ cluster. NH$_3$ is rotating about the axis passing through its center of mass and perpendicular to both the C_3 axis of NH$_3$ and the C_6 axis of benzene.

all three H atoms are equivalent distances from the ring. This latter configuration (**III**) is quite similar to the C_{3v} configuration (**I**), except that NH$_3$ is translationally displaced by ~0.2 Å. The potential energy of configuration **III** is about 10 cm^{-1} higher than that of the stable high-symmetry configuration **I**. In the

rotation of NH$_3$ from configuration **II** to configuration **III**, the cluster passes through a transition state, configuration **IV**, which has a local potential energy maximum. The potential energy difference between configuration **II** and **IV** is only about 10 cm^{-1}. Recall that translational (b$_{xy}$) motions of the NH$_3$ molecule parallel to the benzene plane are of low energy and large amplitude even in the zero-point level of this motion. Therefore, the potential barrier for cluster isomerization from configuration **II** to **I** is ca. 10 cm^{-1}. This cluster's structural isomerization is different from the internal rotational motion described above. One can describe this large amplitude isomerization as a global nonrigidity.

In a supersonic expansion most of the clusters are in their intermolecular zero-point levels, and the barrier to interconversion is barely sufficient to separate the two configurations and render them stable. This assumes that the L-J potential surface is accurate—in any event, the path is of low energy. If the cluster cooling were incomplete, the two isomers should be able to interconvert. Under such conditions of interconversion, a global cluster nonrigidity arises.

HB spectroscopy would be especially interesting for such a system as one could observe different HB spectral features by probing transitions of cluster configurations **I** and **II**. Such spectra would indicate two stable configurations for the benzene(NH$_3$)$_1$ cluster. On the other hand, if the HB spectral features are the same if two different transitions from the two cluster configurations are monitored, interconversion of the two cluster configurations must occur within the lifetime of the experiment (laser pulse resolution, in general). Pico- or femtosecond time resolution for these pump/probe HB studies might yield kinetic information for the isomerization. The interconversion between cluster stable geometries would imply a cluster global nonrigidity.

An additional interesting feature of the L-J potential energy calculations for this cluster is the effect of atomic partial charges on the cluster structure. For the benzene molecule, we adopt the partial charges quoted by Scheraga et al.[30a] in their original work on the L-J−Coulomb potential: $q_C = -q_H = 0.0074\ e$, with e the unit electron charge. The ammonia charges are given as $q_N = -3q_H = 0.351\ e$.[28] If the partial charges on the H and C atoms of benzene all doubled to $q_C = -q_H = 0.015\ e$, the L-J potential calculation yields a single C_{3v} configuration with the same intermolecular separation and a 5 cm^{-1} larger binding energy. With the increase of these partial charges, the local minimum C_s configuration vanishes. Note, however, that for a "fit" potential all the parameters need to be fit together and cannot really be taken as independent. Nonetheless, we clearly see that potential energy calculations must be used with caution and verified by comparison with experimental results.

In the spectra of both benzene(H$_2$O)$_1$ and benzene(NH$_3$)$_1$ clusters extremely low-energy (<10 cm^{-1}) vibronic levels are observed in the 0_0^0 and 6_0^1 transition regions.[5b] These features are not readily assignable to the usual rigid cluster van der Waals vibrational modes. These features are quite likely due to transitions between various contortional (internal rotational) modes in the ground and excited electronic states. MS group analysis must be applied to these systems in order to assign these features and determine the appropriate parameters by which to characterize the cluster nonrigidity.

Ab initio calculations for the benzene(NH$_3$)$_1$ cluster by Cheney et al. use an MP2(FC)/6-31G*//3-21G* approximation[47] and by Brédas and Street use an MP2/6-31G*//3-21G approximation to evaluate cluster strucure and properties.[48] Both calculations generate the most stable cluster structure as one in which the NH$_3$ lies in the plane of the benzene ring with the N

Feature Article

J. Phys. Chem., Vol. 100, No. 32, 1996 **13357**

atom closest to the ring: the N atom apparently forms a hydrogen-bonding structure with the benzene H atoms. The binding energy difference between this in-plane structure and the C_{3v} configuration **I** is ca. 245 and 329 cm^{-1} for the calculations of refs 47 and 48, respectively. Cheney et al. explore the difference in binding energy between configurations **I** and **II** of Figure 5 and find the C_s(**II**) structure more stable than the C_{3v}(**I**) structure by ca. 105 cm^{-1}. Neither group surveyed the global potential energy surface for these clusters so direct information concerning cluster nonrigidity is not available from these ab initio approaches. Both groups do point out that the potential energy surface above the benzene plane is rather flat and that this situation would allow large amplitude bending and torsional motions for small solvent molecules bound at this position.

Extensive experimental and theoretical studies for benzene/ H_2O, NH_3, CH_4 clusters have appeared over the past 10 years. Combining MRES data and L-J empirical potential energy calculations for both benzene(H_2O)$_1$ and benzene(CH_4)$_1$, we can assign a single cluster structure to each cluster. On the other hand, the benzene(NH_3)$_1$ cluster is suggested to have two stable structures. These clusters have solvent molecules above the benzene ring, and the solvent molecules can undergo nearly free rotations about the C_6 axis of benzene: the 6-fold potential barriers for this motion are ca. 1 cm^{-1} or less. Other large amplitude motion can exist in these clusters in addition to the rotation. For benzene(H_2O)$_1$ the in-plane wagging mode has an amplitude of $\pm50°$ even for the zero-point energy level. Exchange of the two water hydrogen atoms in this cluster can be achieved through a concerted motion which involves the out-of-plane torsion mode and the symmetric stretch. In the benzene(CH_4)$_1$ cluster, the exchange of the hydrogen atom away from the ring with the three equivalent ones closest to the ring is unfeasible due to a large hindering potential, and thus the internal CH_4 rotation is one-dimensional and exchanges the three equivalent hydrogen atoms. The two cluster configurations for the benzene(NH_3)$_1$ cluster are separated by a potential barrier of ca. 10 cm^{-1}; isomerization between these two structures is possible. All solvent molecules are able to undergo large amplitude translational motion (±0.5 Å) roughly parallel to the ring even in the zero-point energy level.

Different benzene(H_2O)$_1$ cluster structures are proposed based on vibronic and vibrational data, but the high-resolution microwave results cannot distinguish between them. Both structures with internal motion can generate a symmetric top "averaged" structure. Molecular symmetry group theory is needed to explore these dynamic aspects in greater depth. Ab initio calculations at present do not seem to be as reliable as empirical potential energy calculations for cluster structure, properties, and dynamics.

C. Benzene Dimer. The benzene dimer is of fundamental interest in cluster studies because the pairwise intermolecular exchange interaction between two single aromatic species is difficult to determine. Attempts to extract this information from crystal spectroscopy date back to the mid-1960s.[53] As the physical chemistry community became active in the study of gas phase clusters and van der Waals interactions in general, the benzene dimer was a natural early choice for investigation. We suggest below that nonrigid behavior might be an important component of the inability of the various studies to converge under a single unifying model which can explain all the extant data. The mystery of the benzene dimer structure has attracted many groups to apply different techniques to try to elucidate the cluster structure, but to date no one theory has been employed to explain all the data satisfactorily and generate

unanimous consensus on an unambiguous configuration for the dimer. This is perhaps because a definitive, localized structural solution is as wrong for the benzene dimer as it is for benzene(N_2, CO, CO_2, NH_3, H_2O, CH_4)$_1$ clusters as discussed above. We therefore start this section with a brief review of the experimental and calculational techniques and results employed for the search for a fixed structural solution to the benzene dimer configuration.

Gas phase studies of the benzene dimer began with the work of the Klemperer group[54] in the mid-1970s. They employed molecular beam electric resonance (MBER) techniques with a supersonic nozzle to study the dimer. Since they observed signals, the dimer must have a permanent dipole moment. Assuming that the benzene dimer has a fixed and rigid structure, this result leads to the natural conclusion that the dimer has inequivalent benzene molecules. On the basis of an understanding of the structure of the benzene crystal, they concluded that the dimer has a perpendicular or T-shaped structure. In 1981, the Smalley and Levy groups[55,56] reported MRES, LIF, and DE results for benzene clusters up to the tetramer in both the 0_0^0 and 6_0^1 regions. Hopkins et al.[55] proposed that the benzene dimer rearranges from the ground state (accepted) perpendicular structure to a parallel sandwich structure upon excitation to the first excited electronic state of the cluster. Their conclusion is based on a reduced excited state lifetime, a decreased quantum yield for fluorescence, and broadened transitions for the dimer with regard to the benzene monomer. They suggested that excimer formation occurs in the excited electronic state following the local excited state generation and the dimer's subsequent structural rearrangement. Shinohara and Nishi later argued that the benzene dimer undergoes excimer formation only for S_2 excitation and that the $S_1 \leftarrow S_0$ features observed are not typical for an excimer.[57]

The mass-resolved excitation spectra of isotopically mixed benzene dimers have been obtained by Schauer et al.[58] and by Börnsen et al.[59] for the 0_0^0 and 6_0^1 transitions. H/D substitution for benzene raises the S_1 state 0_0^0 energy by 33 cm^{-1}/D atom or ca. 200 cm^{-1} for C_6D_6. Thus, the resonance exchange interaction is greatly reduced in size and can be extracted in principle from a complete isotopic substitution experiment.[58] The absence of two features/isotopic molecule for the 0_0^0 transition and removal of the 6_0^1 vibronic degeneracy suggest that, unless the site energy differences are less than ~0.1 cm^{-1}, the cluster has equivalent sites of less than 3-fold symmetry. These results, combined with empirical potential energy calculation (of the form exp-6-1 and exp-6-V_{QQ}, V_{QQ} = molecular quadrupole term), led Schauer et al.[58,60] to suggest a parallel displace structure of C_{2h} symmetry, while Schlag et al.[59,61] derived a V-shaped configuration of C_{2v} symmetry.

Scherzer et al.[62] conducted a mass selective hole-burning experiment at the cluster 6_0^1 for isotopically mixed dimers and found two separate structures for the HB experiment. They suggest that the benzene dimer structure is T-shaped. Other weaker bands near the main feature of the homodimer $(C_6H_2)_2$ are found to have a different HB behavior, and these become more prominent with improved cooling conditions: they are assigned as features from "another" cluster structure. Note that the 6_0^1 transition is to a degenerate mode in benzene and thus has some added spectroscopic complication of its own and that two cluster structures seem to be a fairly well "accepted or expected" conclusion.[58,60,62]

More direct probing of the benzene dimer "structure" comes from a study of its rotationally resolved spectra. Gutowsky's group has carried out Fourier transform microwave spectroscopy on this system.[63] On the basis of an assumed T-shaped model

of the dimer in which internal rotation about the axis connecting the centers-of-mass of the two halves of the dimer is essentially free, they fit the microwave data to a symmetric top Hamiltonian with $R_{CM-CM} = 4.96$ Å. The dimer is thought to be quite nonrigid with large tunneling motions interchanging the two benzene molecules. Note that the microwave spectroscopy can only access those dimers with a permanent dipole moment. This study does give evidence for a nonrigid dimer and an averaged symmetric top (C_3 or greater symmetry) configuration.

Raman depolarization ratio measurements have been made for the benzene dimer[18d] for what appear to be two components of the totally symmetric ν_1 mode: drastically different depolarization ratios ($\rho = 0.1$ and 0.02) are found. From the measurement, the two features are assigned as ν_1 modes of two different benzene dimer configurations—one T-shaped ($\rho = 0.1$) and one sandwich ($\rho = 0.02$) structure. Subsequently, Felker et al. suggested that instead of representing two conformers, the two different polarization ratios should be understood to arise from the effect of exchange interactions on the ν_1 mode's isotropic and anisotropic polarizability components. The Felker group also measured Raman transitions for the benzene dimer;[18c,64,65] their results show two bands for each molecular totally symmetric mode for the homodimers (($C_6H_6)_2$ and ($C_6D_6)_2$) and two bands each for the monomer mode for the heterodimer (($C_6H_2)(C_6D_6$)). They thereby conclude that the monomers in the dimer occupy sites of different symmetry—one of high and one of low symmetry. The forbidden 0_0^0 transition in the high-symmetry site accounts for the lack of observed splitting at the dimer 0_0^0 transition, even in the heterodimer.[65] On the basis of the above analysis, they propose a T-shaped dimer configuration in which internal rotation about the axis connecting the molecule centers of mass (perpendicular to one ring and in the plane of the other) is nearly free. This is essentially the same model used by Gutowsky's group.[63]

While the above structural conclusion may be correct, the argument that internal rotation will in some way present an averaged high-symmetry structure for optical transitions that occur in 10^{-16} s ($\Delta E \Delta t \sim \hbar - \Delta t = (5 \times 10^{-12}$ cm^{-1} s$)/4 \times 10^{+4}$ cm$^{-1} \sim 1 \times 10^{-16}$ s) is surely not correct. The proper manner in which to analyze these results is through a complete molecular symmetry group approach as discussed above for benzene(CO, N_2, CO_2, CH_4, etc.)$_1$ and below for the benzyl radical(N_2, $CH_4)_1$ and cyclopentadienyl($N_2)_1$ clusters. The two major problems for the application of molecular symmetry group analysis to the benzene dimer problem are the lack of knowledge of the degree and coordinates of nonrigidity of the cluster and the presumed size of the appropriate MS group. In general, however, such motion should not render an electronic transition forbidden if it were allowed in the absence of the motion; one, of course, need always consider Franck−Condon factors and matrix element size when discussing transition intensity.

Theoretical calculations of the benzene dimer structure and binding energy are also quite numerous for obvious reasons. The review article by Hobza et al.[27] gives a relatively complete account of various calculational results for the benzene dimer. Empirical potential energy calculations have a long history of suggested dimer structures: L-J and exp-6 forms are usually the forms for which most data are fit. Using the exp-6 form, Williams obtained a herringbone structure for the benzene dimer,[66] while Schauer et al. used the exp-6 form with an added molecular quadrupole−quadruple term and obtained a parallel displaced structure.[60] Using partial changes of $|q| > 0.15$ e for each of the atoms, a herringbone structure can also be obtained for the dimer. van der Waal reported the sensitive influence of partial atomic charges on the final structure: increasing the

atomic charges from 0.13 to 0.17 e changes the benzene dimer structure from parallel displaced to T-shaped.[67] Employing the empirical Fraga potential form,[68] Sanchez-Marin et al. investigated various benzene dimer configurations.[69] With a three-center charge model, they found that both the parallel displaced and T-shaped structures are local minima with the parallel displaced one lower in energy (more stable) by ca. 60 cm^{-1}.

On the other hand, most ab initio calculations for the benzene dimer prefer the T-shaped structure, with some degree of nonrigidity.[27,46,52] Reference 70 provides a typical example of such ab initio calculations. MP2 calculations are performed with a small (MIDI-1+s+p) and large (6-31+G*) basis set for various cluster configurations. The most stable structure corresponds to a T-shaped dimer, with intermolecular distance $R_{CM-CM} \sim 5.0$ Å and a binding energy of 944 cm^{-1}. The wagging motion of the stem benzene about the H atom closest to the other benzene molecule is found to be a large amplitude motion. However, with the most extensive basis employed (DZ + 2p) and perhaps then the most reliable, Hobza et al. find four potential minima for the dimer, with the most stable one now being the parallel displaced structure.[71,72] In this configuration the benzene monomers are horizontally displaced by 1.6 Å from the parallel stacked (sandwich) geometry and at a vertical separation of 3.5 Å ($R_{CM-CM} = 3.85$ Å). The parallel displaced structure is ~60 cm^{-1} lower in energy than the T-shaped structure, and the energy barriers separating local minima are quite small.

While theoretical calculations of the dimer structure seem to offer a wide range of choice, the theoretical predictions are still worthwhile. If theory is telling us anything, it surely is saying that the interaction potential between two benzene molecules is quite flat and that many local minima can exist for the dimer. Only small barriers separate parallel displaced, herringbone, and perpendicular (T) configurations. The cluster must have both local (internal rotational) and global (center-of-mass translational motion between local minima) nonrigidity. Clearly, such dynamical behavior will influence the spectroscopic assignments in detail and must be accounted for from the outset through a MS group theoretical analysis. The spectroscopic details that have been assigned to generate structures and number of clusters may only truly reflect the appropriate MS group selection rules for a cluster "without real structure" (i.e., zero-point energy ≈ barrier heights separating local potential minima). We explore this nonrigidity below by varying the parameters for a simple intermolecular potential form (L-J−Coulomb) because it represents a typical set of theoretical results.

The simplest L-J (6−12) empirical calculation without an electrostatic interaction term yields a single potential minimum which corresponds to a parallel staggered dimer structure (D_{6d} symmetry). (See Figure 7 for all the various dimer possible structures.) The intermolecular distance R_{CM-CM} is 3.38 Å, and the calculated binding energy is 1646 cm^{-1}. The experimental value for the binding energy of the dimer is 70 meV (~565 cm^{-1}),[73] which is based on an MPI study of the benzene cluster dissociation process. All the calculated dimer binding energies seem to far exceed this value. The internal rotation of this dimer configuration about the C_6 axis results in a small 6-fold potential with a barrier height of ~8.5 cm^{-1}. The doubly degenerate van der Waals torsional motion of one benzene monomer rotating around an in-plane axis is calculated to be small amplitude vibration, whose potential well is much steeper than that of the other benzene/X clusters discussed above. Therefore, this benzene dimer configuration can undergo one-dimensional internal hindered rotation with the barrier height of 8.5 cm^{-1}. The doubly degenerate van der Waals bending mode of this

Feature Article

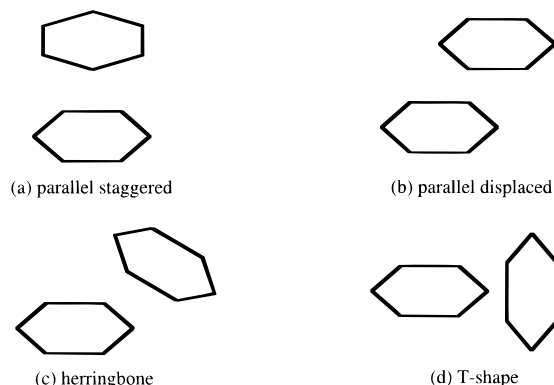*J. Phys. Chem., Vol. 100, No. 32, 1996* **13359**

Figure 7. Schematic diagram of the four different benzene dimer configurations: (a) parallel staggered, (b) parallel displaced, (c) herringbone, and (d) T-shape. With the variation of the atomic partial charges, all these four dimer geometries are possible potential minimum configurations in the L-J−Coulomb empirical potential calculations. The C−H bonds are omitted here for simplicity.

dimer configuration is additionally a large amplitude motion. The parallel sliding motion of the two monomers has a large amplitude of $\sim\pm0.5$ Å even at the zero-point energy level. Other configurations (T-shaped, parallel displaced, herringbone) do not correspond to potential minima. The potential energy of the T-shaped configuration is at least 1000 cm^{-1} higher.

The benzene molecule has no permanent dipole moment due to its D_{6h} symmetry, and therefore the molecular quadrupole−quadrupole interaction term V_{QQ} is the first nonzero term in a multipole expansion of intermolecular electrostatic interaction for a dimer. It plays an important role in determining the cluster structure and stabilization energy. Schauer et al., employing exp-6 + V_{QQ} potential form, obtained a single stable dimer configuration of parallel displaced structure with C_{2h} symmetry;[60] however, the quadrupole moment value, $Q = 5.6 \times 10^{-26}$ esu cm^2, used in that calculation was quoted from a 1969 paper,[74] which is just about $^1/_2$ of the value, $Q = -10.0 \times 10^{-26}$ esu cm^2, obtained later with more accurate measurements.[75] Using the updated quadrupole moment value in the V_{QQ} term,[76] we recalculate the dimer structure with the L-J + V_{QQ} potential form. The only potential minimum still corresponds to a parallel displaced configuration with C_{2h} point group symmetry, with the center-of-mass displacements $\Delta Z = 3.06$ Å, $\Delta X = 2.50$ Å, and $\Delta Y = 0$. The calculated binding energy is 2058 cm^{-1} using this larger value of Q: the old quadrupole moment value ($Q = -5.6 \times 10^{-26}$ esu cm^2) yields a binding energy of 1492 cm^{-1}. This parallel displaced configuration is more rigid than the parallel stacked one, with a 6-fold potential barrier of about 40 cm^{-1} for the internal rotation of benzene around its C_6 axis. The internal rotation of benzene around its in-plane axis (x or y) is highly hindered. To probe the influence of the molecular quadrupole interaction on the dimer properties, we varied the benzene quadrupole moment by 2 orders of magnitudes (from $Q = -5.6 \times 10^{-27}$ to $Q = -5.6 \times 10^{-25}$ esu cm^2); the results of these calculations are listed in Table 3. All values of the benzene quadrupole moment lead to a parallel displaced dimer configuration, which is the only stable structure on this entire potential energy surface. With the increase of the quadrupole moment, the Z displacement drops monototically, while the X displacement experiences first an increase and then a decrease.

A multipole expansion of a system's electrostatic potential can be truncated at the first several terms only if the field distance (in our dimer case, the intermolecular distance) is much larger than the system's dimension. Apparently, the benzene dimer does not meet this criterion, as the intermolecular distance (~5 Å) is about the same as the size of benzene molecule. Even

though the octupole of benzene molecule vanishes due to the D_{6h} symmetry, higher terms such as the hexadecapole still play an important role in the multipole expansion of the electrostatic interaction energy. This point has been addressed by Klemperer et al. before.[54a]

A better way to account for the nonbonded electrostatic interaction in empirical potential energy calculations is to employ atom−atom pairwise additive Coulomb interactions between the partial charges at each atomic site. The atomic partial charges in benzene are treated equally as $q_C = -q_H = q$. The actual value of q, of course, can have many possibilities. We have in the past used Sheraga et al.'s result $q = 0.0074$ e obtained from CNDO/2 calculations,[30a] since with this q value they successfully calculated the conformations (secondary structure) of many large molecules;[77] however, this value is now thought to be quite an underestimate of q. Even so, q must be seen as a parameter in a L-J−Coloumb potential and as such is probably not independent of the other parameters. Williams[66] and van der Waal[67] both used $q = 0.153$ e, which is the parameter fit to the crystal structures and agrees well with modern ab initio and modeling estimates ($0.10 \leq q \leq 0.20$).

For Z-axis cylindrically symmetric systems like benzene, the nonzero quadrupole moment components are $Q_{ZZ} = -2Q_{XX} = -2Q_{YY} = Q$. With $q_C = -q_H = q$ and the benzene bond lengths, a third set of partial charges $q = 0.165$ e for $Q = -10.0 \times 10^{-26}$ esu cm^2 (or $q = 0.0925$ e for $Q = -5.6 \times 10^{-26}$) can be suggested. All these q values vary by more than a factor of 20, so we again perform a series of L-J−Coulomb empirical potential energy calculations over an appropriate range of partial atomic charges. When q is relatively small (≤ 0.09 e), the Coulomb interaction term is quite insignificant. Only one stable dimer configuration exists which is the same as the L-J calculational result: a parallel staggered structure. With the increase of q, the cluster binding energy gradually decreases from 1646 cm^{-1} ($q = 0$) to about 1431 cm^{-1} ($q = 0.0925$ e, which corresponds to a quadrupole moment of $Q = -5.6 \times 10^{-26}$),[75] while the intermolecular distance increases from 3.38 to 4.00 Å. When $q > 0.093$ e, a second stable configuration emerges which corresponds to a parallel displaced structure of C_{2h} point group symmetry. The two benzene monomers in the parallel staggered configuration tend to slip parallel to each other as q increases. The vertical (Z) separations of the two benzene monomers are about 3.39 and 3.37 Å for the parallel staggered and parallel displaced configurations, respectively. The calculated binding energies of both configurations continue to decrease. At $q = 0.1$ e, the binding energies of both configurations are almost the same. The horizontal displacement of the parallel staggered configuration increases from 0.066 Å ($q = 0.0925$ e) to 0.54 Å ($q = 0.1$ e). The interchange of these two configurations involves a 30° internal rotation of one benzene monomer around its C_6 axis and some short-distance translations ($\Delta Z \approx 0.02$ Å, $\Delta Y \approx 0.28$ Å). The energy barrier between these two configurations is estimated to be around 10 cm^{-1}, and thus a global nonrigidity exists for the benzene dimer at 0.093 $e < q \leq 0.1$ e.

With $q > 0.1$ e, the parallel staggered configuration no longer corresponds to a potential minimum but becomes a saddle point, and the benzene dimer has again only one stable structure−the parallel displaced configuration. With the further increase of q, this parallel displaced configuration starts to evolve toward the herringbone structure, in which the two displaced benzene monomers are no longer parallel to one another. The dimer binding energy experiences a minimum (~1100 cm^{-1}) at about $q = 0.2$ e and then increases again. When $q \geq 0.3$ e, this herringbone structure evolves toward a T-shaped configuration

TABLE 3: Benzene Dimer Structures with L-J $+ V_{QQ}$ Empirical Potential Energy Calculations

	quadrupole moment Q (esu cm^2)					
	5.6×10^{-27}	2.8×10^{-26}	5.6×10^{-26}	1.0×10^{-25}	2.8×10^{-25}	5.6×10^{-25}
dimer configuration	parallel displaced	parallel displaced	parallel displaced	parallel displaced	parallel displaced	parallel displaced
Z displacement ΔZ (Å)	3.38	3.29	3.19	3.06	2.60	2.13
X displacement ΔX (Å)	0.25	1.68	2.27	2.50	2.25	1.85
binding energy E_b (cm^{-1})	1614.6	1430.0	1492.3	2057.8	12736	104064

TABLE 4: Summary of the L-J−Coulomb Calculational Results for the Benzene Dimer

partial charge q (e)	dimer configuration(s)[a]	binding energy E_b (cm^{-1})	
0.0074[b]	ps	1644.1	
0.05	ps	1582.5	
0.08	ps	1485.0	
0.0925[c]	ps	1431.5	
0.095	ps	1419.9	
	pd		1418.1
0.10	ps	1396.6	
	pd		1396.4
0.105	pd	1374.1	
0.153[d]	pd	1156.8	
0.20	h	1098.6	
0.28	h	1284.6	
0.30	T	1363.8	
	pd		1317.9
0.40	T	1884.6	
	pd		1777.7
0.50	T	2435.4	
	pd		2649.8
0.75	T	5047.1	
	pd		5644.7

[a] The configurations are ps = parallel staggered, pd = parallel displaced, h = herringbone, and T = T-shaped. [b] Reference 30. [c] Corresponds to a quadrupole moment of -5.6×10^{-26} esu cm^2, ref 74. [d] References 66 and 67.

in which the two benzene monomers are nearly perpendicular to each other. At the same time, another stable dimer structure emerges which corresponds to a parallel displaced configuration. At $q = 0.3$ e, the nearly T-shaped herringbone configuration has a binding energy of 1363 cm^{-1}, while the parallel displaced configuration is a little less stable at 1318 cm^{-1}. With the further increase of q, the calculated binding energies of both configurations keep growing to unreasonably large values. Table 4 gives a brief summary of the calculation results with different q values.

In general, the dimer binding energy encounters a minimum at about $q = 0.2$ e, and even this minimum binding energy (1100 cm^{-1}) is much larger than the experimentally derived value (565 cm^{-1}).[73] The updated quadrupole moment value (-10.0×10^{-26}) corresponds to an atomic partial charge of $q = 0.165$ e, while the value $q = 0.153$ e cited in refs 66 and 67 is derived from the crystal structure. From these results we believe that $q > 0.3$ e is an overestimate, and the best-fit value of q could be between 0.1 and 0.2 e. At $q = 0.15$ e, the benzene dimer is calculated to be of a parallel displaced geometry, with a binding energy of 1170 cm^{-1}. The parallel (Y) and the vertical (Z) displacements between the two benzene monomers are 1.72 Å and 3.32 Å, respectively. These results can be compared with those from the ab initio calculations;[72] with their largest basis set, Hobza et al. find the most stable benzene dimer structure has a parallel displaced geometry, a stabilization energy of ~800 cm^{-1}, and horizontal and vertical displacements of 1.6 Å and 3.5 Å, respectively.[71,72] With smaller basis sets, a T-shaped geometry is found to be the most stable dimer configuration. In the empirical potential energy calculations, only when 0.3 e < q < 0.4 e is the T-shaped dimer more stable than the parallel displaced dimer. The van der Waals bending modes (b$_x$, b$_y$)

represent the parallel slipping of the two benzene monomers and are calculated to be large amplitude motions.

In addition to the structure variations and global nonrigidity discussed above as q is varied, local nonrigidity (internal rotation of benzene) exists in all dimer configurations within the L-J−Coulomb calculations. For example, for $q = 0$ the parallel staggered dimer has a 6-fold internal rotation barrier of 8.5 cm^{-1}, while for $q = 0.15$ e the 6-fold barrier to internal rotation in the parallel displaced configuration is 4.1 cm^{-1}. At larger q (~0.25 e), the tilted benzene monomer of the herringbone configuration has a barrier to rotation about its 6-fold axis of ~14 cm^{-1}, while the bottom monomer of this structure has a barrier to rotation of about 600 cm^{-1}. This same disparity exists for the T-shaped dimer in which the top benzene can rotate freely about its C_6 axis and the stem cannot. Figure 7 displays these various structures.

In conclusion, L-J, exp-6, and other empirical potential energy calculations have been conducted for the benzene dimer cluster. The electrostatic interaction term plays an important role in determining cluster structure. Using a molecular quadrupole−quadrupole interaction term always yields a single potential minimum of parallel displaced geometry. The electrostatic interaction can be modeled with Coulomb interaction between the atomic partial charges of the two benzene monomers. Structure of the dimer is quite sensitive to partial charge values chosen, and multiple stable configurations can arise. When 0.09 e < q < 0.1 e, two stable dimer configurations (parallel staggered and parallel displaced) exist. Isomerization between these two configurations indicates global nonrigidity for the benzene dimer. The best estimate of q is ~0.15 e, which results in a parallel displaced stable structure with a binding energy of ~1170 cm^{-1}. The internal rotation of one benzene monomer around its C_6 axis is slightly hindered in this structure, and this is the only cluster nonrigidity behavior at this q value. With increase of q, the benzene dimer experiences a structural change from parallel staggered to parallel displaced, to herringbone, and finally to T-shaped at its potential minimum.

Experimental results for the dimer structure are also somewhat ambiguous in that a number of configurations have been identified. The T-shaped geometry is probably the most often suggested at present, but parallel displaced and herringbone structures are not without their supporters and have not been ruled out. In fact, theory and experiments are in pretty fair agreement: the cluster is definitely nonrigid in both rotational and translational coordinates, and the structure is not well defined or determined except in an averaged sense. We believe that the calculations taken in total faithfully represent the dimer's nonrigidity, the flatness of its potential surface, and the sensitivity of its structure to small changes in potential forms, parameters, and ab initio calculational algorithms. Clearly, the next step for this system is an analysis of the nonrigidity problem through molecular symmetry group theory. The only extant experimental value for the dimer binding energy (565 cm^{-1}) is probably small by a factor of 2 or 3.

D. Toluene/N$_2$, H$_2$O, NH$_3$, CH$_4$. MRES and empirical potential energy calculations have been carried our for toluene clustered with a number of small solvent molecules;[78−81]
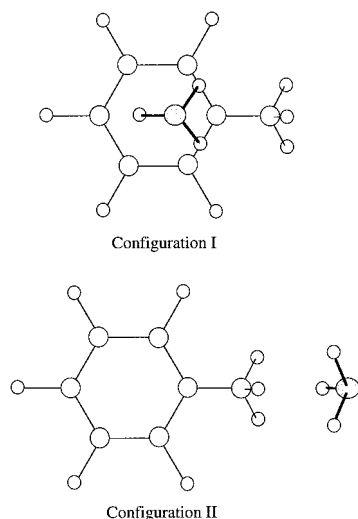
Feature Article

J. Phys. Chem., Vol. 100, No. 32, 1996 **13361**

Configuration I

Configuration II

Figure 8. Schematic diagram of the two toluene(NH_3)$_1$ cluster configurations. In configuration **I** the NH_3 is ~3.2 Å on top of the phenyl ring with the three H atoms closer to the ring plane. In configuration **II** the NH_3 lies close to the methyl group of toluene, with the three H atoms closer to the phenyl ring. The C_3 axis of NH_3 overlaps with the principal axis of toluene.

nonetheless, cluster nonrigidity has not been considered for any of these systems. With the methyl group addition to the benzene ring, cluster symmetry is greatly reduced with respect to that for benzene clusters, and the hindering potential for both rotations about the former high-symmetry ring axis and large amplitude translational motion should be increased. Therefore, one can expect that toluene clusters with N_2, H_2O, NH_3, and CH_4 solvent molecules will behave somewhat differently from the comparable benzene cluster. In the discussion below we present new calculations that address specifically the question of large amplitude internal motion for these clusters. We continue to use the L-J−Coulomb (6−12−1) potential form because other potentials seem to yield the same general results and to reach the same general conclusions.

We have recalculated the cluster structure and potential surface for toluene (N_2, H_2O, NH_3, CH_4)$_1$ clusters using the L-J−Coulomb potential forms. All forms of these 1 to 1 clusters have similar calculated structures with two local potential minima: one local minimum is with the small molecule solvent above the ring in much the same conformation as described above for benzene clusters (configuration **I**), and the second equilibrium structure has the small solvent molecule lying in the plane of the toluene ring and coordinated to the CH_3 group of toluene (configuration **II**). Using toluene (NH_3)$_1$ as an example, Figure 8 schematically displays these two cluster isomers. The binding energy for configuration **I** is typically 3 times that of configuration **II**. In configuration **I** (the only cluster observed in experiments reported thus far) the center of mass of the solvent molecule is shifted from above the ring center position toward the methyl group. All the AH$_n$ (A = C, N, O) solvent molecules have their centers of mass nearly above the toluene center of mass (about 0.5 Å from the center of the ring toward the methyl group). In the case of toluene(N_2)$_1$ the horizontal displacement of N_2 toward the methyl group is ~0.33 Å. The hydrogen atoms of H_2O and NH_3 are closer to the ring than the N or O heavy atoms, and CH_4 has three hydrogen atoms close to the ring and the fourth further away than the carbon atom. These structures manifest again the general hydrogen-bonding interaction between the negative ring π-system and the somewhat positive hydrogen atoms of the solvent. In configuration **II** the centers of mass of the solvent molecules lie on the C_2 principal axis of toluene with an intermolecular center-

TABLE 5: Calculated Cluster Configurations, Binding Energies, Intermolecular Distances, and Potential Barriers for Solvent Internal Rotation Employing a L-J−Coulomb Potential

cluster	config[a]	binding energy E_b (cm^{-1})	intermolecular distance R_{CM-CM} (Å)	internal rotation potential barrier (cm^{-1})
toluene(N_2)$_1$	T	550.3	3.31	6.6
	S	192.7	5.98	
toluene(H_2O)$_1$	T	668.0	3.38	71.3
	S	197.5	5.78	
toluene(NH_3)$_1$	T	851.2	3.22	20.5
	S	256.6	5.92	
toluene(CH_4)$_1$	T	591.2	3.46	14.6
	S	215.3	6.11	

[a] T = on top of the aromatic ring; S = on the C_2 axis of toluene, at the methyl group side.

of-mass distance of about 6 Å or about 3.5 Å from the methyl group. Table 5 summarizes the calculated binding energies and intermolecular distances for these cluster configurations.

These calculations must assume a geometry for the toluene methyl rotor even though one does not properly exist. If the geometry is chosen to be asymmetric, the binding energy for the two possible ring centered isomers differ by ca. 10 cm^{-1}. These two energies are averaged to obtain the numbers in Table 5. Alternately, one can use a symmetric methyl structure (one C−H bond in the ring plane). For the solvent at the ring position a 2-fold barrier to rotation for H_2O and N_2 and a 3-fold barrier to rotation for NH_3 and CH_4 can be identified. Values for these potential barriers are given in Table 5. The H_2O 2-fold barrier is large (~70 cm^{-1}), but the other barriers are small and should allow weakly hindered rotation of the solvent to occur. Both torsional motion of the solvent and translation of the solvent over the ring (bends) are of large amplitude.

In configuration **II**, the N_2 molecule bond axis lies perpendicular to the C_2 axis of toluene, and the other solvents of the form AH$_n$ (A = C, N, O) have their hydrogen atoms toward the methyl group of toluene to the maximum extent. The internal rotation of the toluene methyl group coupled with the solvent rotation about the toluene C_2 axis will generate a complex problem that must be treated within the context of molecular symmetry group theory. Large amplitude motion will also occur for solvent molecule translation perpendicular to the toluene C_2 axis. One must keep in mind, however, that this latter cluster has never been observed, and with a factor of 3 difference in the local potential energy minima for these clusters, one would not expect the high-energy cluster to be stable in the cooling process.

In summary, toluene clusters with N_2, H_2O, NH_3, and CH_4 are calculated to have two stable configurations: one has the solvent molecule above the aromatic ring plane, and the other places the solvent molecule on the C_2 axis of toluene, close to the methyl group. The binding energies of the first configuration are much larger than those of the second configuration. In the first configuration, the solvent molecules shift from the ring center toward the methyl group and are able to rotate about the axis perpendicular to the ring plane. This one-dimensional rotor has a higher potential barrier than the related benzene cluster due to interaction of the solvent molecule with the toluene methyl group. In the second configuration, the internal rotation of the solvent molecule would couple with the methyl rotor of toluene to make the cluster energy level scheme even more complicated.

E. Aniline/N_2, H_2O, NH_3, CH_4. The aniline molecule ($C_6H_5NH_2$) has a reasonable vapor pressure and a large extinction coefficient for the $S_1 \leftarrow S_0$ electronic transition and

has thus been the focus of a number of supersonic jet laser experiments. We studied aniline/He, CH_4 clusters a number of years ago.[9,82] The aniline$(CH_4)_1$ cluster spectrum shows a strong 0_0^0 transition that is broad (fwhm ~8 cm^{-1}) and is composed of at least three unresolved features. Although not assigned at the time, one can now suggest that these features are associated with internal rotational transitions of the CH_4 with respect to the ring.[9] Calculation suggests that the minimum-energy structure for this cluster is the same as that for benzene and toluene/CH_4 clusters. Aniline/Ar, N_2, CH_4 clusters have also been studied with regard to their dynamics.[82] Coutant and Brechignac observed aniline/$H_2(D_2)$ clusters for the $S_1 \leftarrow S_0$ transition in the 0_0^0 region and fit the resulting spectrum to a nearly free internal rotor model.[83] Aniline offers an opportunity for the study of hydrogen bonding between the NH_2 group and the solvent H atoms and NH_2 group H atoms and the solvent O and N atoms.

According to microwave spectroscopy results,[84] the two H atoms of the amino group of aniline are below the phenyl ring plane by an angle of ~39.4°, with the H−N−H angle about 113.9°. The pyramidal structure of the amino group makes the two sides of the ring plane inequivalent; thus, the binding energies of the solvent molecule above and below the ring plane are also slightly different. In aniline$(N_2)_1$, the N_2 bond axis lies nearly parallel to the mirror plane of aniline, with an intermolecular distance of $R_{CM-CM} \sim 3.30$ Å. The N_2 center of mass is shifted from the ring center toward the amino group and nearly coincides horizontally with the center of mass of aniline. Internal rotation of N_2 about the out-of-plane axis has an apparent 2-fold potential. The barrier height and the cluster binding energy are 13.0 and 555 cm^{-1}, if the N_2 is on the same side of the ring as the two amino hydrogens, or 6.3 and 538 cm^{-1}, if they are on different sides of the ring plane. In both cases, the N_2 is a slightly hindered, one-dimensional internal rotor in the aniline$(N_2)_1$ cluster.

A similar case can be found for the aniline$(CH_4)_1$ cluster. The calculated aniline$(CH_4)_1$ cluster structure has the CH_4 molecule either above or below the ring plane, with three H atoms closer to the phenyl ring and the fourth H further away than the carbon atom of CH_4. The center of mass of CH_4 is about 3.4 Å above or below the ring plane and horizontally shifted from the ring center toward the amino group. The internal rotation of CH_4 around the out-of-plane ring axis is pseudo-3-fold, with the potential barrier ~9.8 cm^{-1} if the CH_4 and the two amino hydrogens are on the same side of the ring plane or ~1.5 cm^{-1} if they are on different sides of the ring. The binding energy of this cluster is also slightly dependent on the side of the ring that CH_4 occupies: 573 cm^{-1} for the opposite side of the ring from the amino group H atoms and 595 cm^{-1} for the same side of the ring as the amino group H atoms. The torsional motion of CH_4 about an axis parallel to the ring plane is greatly hindered by a potential barrier of at least 300 cm^{-1}; therefore, the CH_4 internal rotation is only one-dimensional.

The cases for aniline$(H_2O)_1$ and aniline$(NH_3)_1$ are more complicated due to the hydrogen-bonding interaction of the solvent molecule with the amino group of aniline. Empirical simulation shows that both 1:1 clusters have four local potential minima: two correspond to the usual van der Waals cluster for which the solvent molecule is either above or below the ring plane, and two correspond to hydrogen-bonding clusters for which the hydrogen bond occurs either between the amino hydrogen of aniline and the N or O atom of the solvent molecule or between the protons of the solvent molecule and the amino N atom of aniline. In the first class of clusters (solvent molecule either above or below the ring plane), cluster configuration is
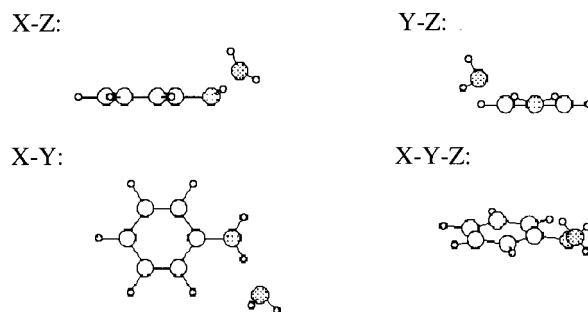

Figure 9. Schematic diagram of one of the H-bond clusters of aniline-$(H_2O)_1$. The H_2O is near the amino group of aniline, and the H-bond is between the lone pair electrons of O atom of H_2O and the proton of the amino group of aniline.
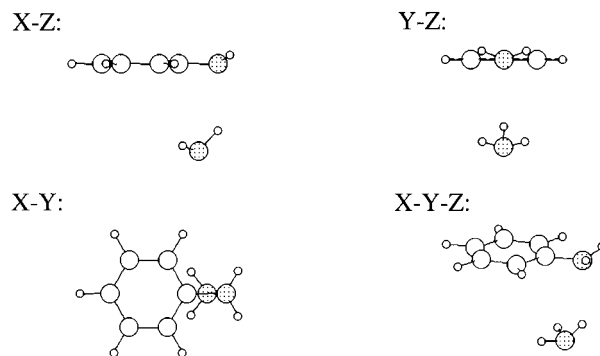

Figure 10. Schematic diagram of one of the H-bond clusters of aniline-$(NH_3)_1$. The NH_3 is near the amino group of aniline, and the H bond is between the lone pair electrons of N atom of the amino group of aniline and one proton of NH_3. The other two hydrogen atoms of NH_3 are drawn toward the phenyl ring by the attractive interaction with the π-electron system.

similar to that of aniline$(N_2)_1$ and aniline$(CH_4)_1$ clusters. The intermolecular distances are about 3.4 and 3.3 Å, and the binding energies are about 670 and 820 cm^{-1} for the aniline$(H_2O)_1$ and aniline$(NH_3)_1$ clusters, respectively. The asymmetric nature of the amino hydrogens with respect to the ring plane causes only small inequivalences. For example, the binding energies for the solvent molecule above and below the ring plane differ by only ~11 cm^{-1} in aniline$(H_2O)_1$ and ~7.6 cm^{-1} in aniline-$(NH_3)_1$. The internal rotation of NH_3 about the out-of-plane axis is nearly free, with the potential barrier of only about 2.5 cm^{-1}. On the other hand, the H_2O solvent molecule is more confined by a hindering potential of at least 66 cm^{-1}. Therefore, the H_2O can only have large amplitude vibration about the out-of-plane axis, with its equilibrium geometry symmetric to the mirror plane of the aniline.

The second type of aniline cluster, hydrogen-bonded cluster configurations, are more interesting. The hydrogen bond occurs either between the amino hydrogens and the lone pair electrons of N or O atom of the solvent molecule or between the protons of the solvent molecule and the lone pair electrons of the amino N atom of aniline. Therefore, two different hydrogen-bonded cluster configurations can occur for each cluster. Depending on the strength of various interactions, the actual cluster structure turns out to be a balanced compromise of all the interaction component types. Figures 9 and 10 show the most stable hydrogen-bonded cluster structures for aniline$(H_2O)_1$ and aniline$(NH_3)_1$, respectively. In the aniline$(H_2O)_1$ cluster shown in Figure 9, the hydrogen bond is between the lone pair electrons of O atom and the amino hydrogen of aniline. The binding energy of this configuration is 1207 cm^{-1}, which is more than twice as large as the other hydrogen-bonded cluster (595 cm^{-1}) in which the H bond occurs between the solvent proton and the

Feature Article

J. Phys. Chem., Vol. 100, No. 32, 1996 **13363**

amino N atom of aniline. This implies that the O···H hydrogen bond is the dominant interaction in the cluster. On the other hand, in the aniline(NH$_3$)$_1$ cluster, the two hydrogen-bonded configurations have almost the same binding energies, 720 and 719 cm^{-1}, as the hydrogen bonds in both cases are of the N···H type. These two binding energies are lower than those of the cluster configurations in which the NH$_3$ molecule is either above or below the ring plane. For aniline(NH$_3$)$_1$ (Figure 10), the hydrogen bond is between the amino group N atom and the proton of the NH$_3$ solvent molecule. The two other H atoms of NH$_3$ are attracted toward the phenyl ring of the π-electron system. Due to hydrogen-bonding interactions, the solvent molecule in each cluster configuration is rigid, and no internal rotation occurs at low temperature.

In both the aniline(H$_2$O)$_1$ and aniline(NH$_3$)$_1$ clusters, interchanges of different configurations are strongly prohibited; that is, global nonrigidity does not exist. The barrier to such internal motions comes mostly from the amino group, for which the strong interaction not only prevents the solvent molecule from migrating from the above (below)-ring-plane position to hydrogen-bonded/end position but also prohibits the interchange of the two hydrogen-bonded cluster configurations. Therefore, according to the empirical potential calculations, each cluster should have four rigid isomer conformations. Experimental verification of this prediction should be quite challenging and will surely take a number of different approaches to prove conclusively.

In conclusion, due to the pyramidal nature of the amino group of aniline, the aniline(N$_2$)$_1$ and aniline(CH$_4$)$_1$ clusters can have their solvent molecule on either the same or opposite side of the ring as the NH$_2$ hydrogen atoms. The binding energy and the internal rotation barrier are slightly different in each case. Both clusters exhibit one-dimensional internal rotation. In aniline(H$_2$O)$_1$ and aniline(NH$_3$)$_1$ clusters, besides the two cluster configurations in which the solvent molecule is either above or below the ring with respect to the amino group, two more cluster configurations exist corresponding to dominant hydrogen-bonding interactions either between the solvent proton and the lone pair electrons of the amino N atom of aniline or between an amino hydrogen and the solvent N or O atoms. The O···H hydrogen bond interaction is the strongest for these clusters. The strong interaction between the amino group and the solvent molecules prevents the interchange of different cluster configurations, and thus no global nonrigidity is possible for the aniline/H$_2$O, NH$_3$ system.

F. Radical Clusters. One of the main motivations behind the study of clusters is to understand the nature of solvation and how it changes the physical, dynamical, and chemical properties of molecules. As the application of supersonic expansions and the various laser spectroscopy techniques have turned to reactive intermediates,[5c,d,85−87] interest has also turned to the solvation behavior of these transient species. Indeed, the expectation is that the solvation properties of transient species (radicals, carbenes, nitrenes) should be even more varied and interesting than those of stable molecules. The aromatic radicals we have studied are benzyl radical (BR),[5c,87] cyclopentadienyl (cpd),[5d] CN-cpd,[87] and others.[88] These radicals form stable clusters with many of the solvents used to study solvation of stable molecules, and their clusters also display nonrigid behavior. In this section we will discuss a few representative systems (BR/N$_2$, CH$_4$, and cpd/N$_2$) for aromatic reactive intermediates to demonstrate even further the generality of nonrigid cluster behavior.

The MRES spectra of BR clustered with Ar, N$_2$, and C$_n$H$_{2n+2}$ ($n = 1−3$) solvent molecules have been reported earlier.[5c] Three

electronic states 1^2B_2 (D$_0$), 1^2A_2 (D$_1$), and 2^2B_2 (D$_2$) of the BR are involved in the electronic excitation. Ab initio calculations (CASSCF) can be employed to obtain BR transition energies and structure for these three states. With the information on BR structure and the atomic partial charges in hand, exp-6−Coulomb empirical potential energy calculations can be performed on the radical clusters. Different sets of empirical parameters are used for the three electronic states to reproduce the cluster spectral shifts. BR has a planar structure, and the BR(N$_2$)$_1$ cluster has a single potential minimum which has the N$_2$ placed above and parallel to the aromatic ring plane. The calculated binding energies are around 530 cm^{-1} for the three electronic states, which is somewhat larger than the experimental value.[5c] The exact positions of the N$_2$ are different for these three states: in D$_0$ and D$_1$, the N$_2$ bond axis is perpendicular to the C_2 axis of BR, while in D$_2$, the N$_2$ bond axis is parallel to the C_2 axis of BR. Compared to the D$_0$ state, the calculated N$_2$ position in D$_1$ state is shifted 0.07 Å toward the CH$_2$ group end. The internal rotation of N$_2$ about an axis perpendicular to the BR plane is slightly hindered by a 2-fold potential barrier. The barrier heights modeled from the experimental results are 13 cm^{-1} in the ground state and ∼17 cm^{-1} in the mixed excited states. Large amplitude motions are also found for the N$_2$ bending modes in which the N$_2$ at the zero point energy level is able to translate ±0.4 Å across the aromatic plane.[5c]

The BR/CH$_4$ cluster structure is more complicated. In D$_0$ and D$_1$ states, the calculated stable cluster configuration places CH$_4$ in an asymmetric position near the α-carbon of BR.[5c] This creates a double-minimum potential well which is symmetric about the σ_v plane perpendicular to the BR. Isomerization between these two local potential minima involves the cluster van der Waals bending mode with the CH$_4$ moving perpendicular to the C_2 axis of BR: this motion has a low barrier. Therefore, global nonrigidity exists in this double-well BR(CH$_4$)$_1$ cluster. Two H atoms of CH$_4$ are tilted toward BR plane, but neither 2-fold nor 3-fold rotational symmetry is preserved for CH$_4$ in this cluster configuration. In the D$_2$ state, the BR(CH$_4$)$_1$ cluster has a stable configuration similar to the An(CH$_4$)$_1$ case, in which the CH$_4$ is placed symmetrically on top of BR with three H atoms equally close to the ring plane. The binding energies calculated for the three electronic states vary from 500 to 550 cm^{-1}, which is consistent with the experimental observations. Employing empirical potential energy calculations, the lowest potential barriers for the 3-fold CH$_4$ internal rotation are found to be 21.5, 32.6, and 136.5 cm^{-1} for the D$_0$, D$_1$, and D$_2$ states, respectively, while the 2-fold internal rotations have even higher hindering potential (>200 cm^{-1}). Vibronic transitions, on the other hand, indicate that the internal rotations are nearly free, and both 3-fold and 2-fold rotation models fit the spectra and yield barrier heights ≤3 cm^{-1}. A three-dimensional rotor model is probably necessary to analyze the spectral features associated with the CH$_4$ internal rotation in the BR(CH$_4$)$_1$ cluster.

The cpd radical is planar and has D_{5h} point group symmetry. The D$_1$ ← D$_0$ excitation spectrum of cpd(N$_2$)$_1$ at the 0_0^0 region shows three groups of transitions which are assigned as a Franck−Condon progression of the van der Waals out-of-plane stretch mode of ∼55 cm^{-1}. Each group of transitions contains three partially resolved peaks separated by about 3 and 9 cm^{-1}. HB experiments indicate that the two outside peaks originate from a same vibrational level in the ground state while the center peak is from another level. These features are assigned as the vibronic transitions between different internal rotation levels in the D$_0$ and D$_1$ states.[5d] Employing L-J−Coulomb empirical potential energy calculations, the stable configuration of

cpd(N_2)$_1$ is found to have the N_2 symmetrically on top of the cpd radical with its bond axis parallel to the ring plane; the two centers of mass are at an intermolecular distance of 3.36 Å, and the cluster has a binding energy of 434 cm^{-1}. The internal rotation of N_2 about the intermolecular axis yields a 10-fold potential barrier with a height of less than 0.01 cm^{-1}. The spectral fit of the rotor level transitions indicates that the potential barrier in the D$_1$ excited state is also quite low. The D$_{5h}$(MS) group is generated to analyze the free rotor spectra. The optical selection rules derived exclude transitions between even and odd internal rotor levels, thus explaining the two groups of transitions in the HB experiment.[5d]

V. Conclusions

We have discussed more than a dozen systems for which nonrigid cluster behavior is found either experimentally or predicted based on model potential energy calculations. Even though the discussion has been limited to 1:1 aromatic/solvent clusters, one can still conclude from these studies that cluster nonrigidity is more the rule than the exception. Two types of nonrigid behavior of clusters have been emphasized: coexistence of multiple stable configurations that interconvert through internal rotational motion and large amplitude translational motion. The latter motion is present in almost all van der Waals clusters studied to date. One should no longer think of a van der Waals cluster as a rigid entity with a well-defined structure; a van der Waals cluster is a dynamic system for which structure is best considered an averaged attribute. This concept brings with it other changes in approach, the most fundamental of which is the evolution from point group theory to molecular symmetry group theory for level classifications and Hamiltonian diagonalization.

Cluster nonrigidity surely has an impact on the cluster structure identification process. Cluster nonrigidity must be considered in spectral analysis (energy level identification) and in theoretical modeling of clusters. On the other hand, we often need a reference structure (any shallow local energy minimum on the cluster global potential surface) from which nonrigid characteristics and large amplitude motion can be built and evaluated. The interplay of cluster nonrigidity and cluster structure further complicates the problem of cluster characterization. The benzene dimer is perhaps one of the best examples of this interaction and complexity. Every suggested dimer structure has a significant degree of nonrigidity, and the nonrigid nature of the cluster makes many structural possibilities plausible. To break this loop one must view the dimer as a dynamic system rather than one with a well-defined structure. In reality, the benzene dimer probably is accessing a number of different local minima due to large amplitude motion. The final solution to this problem comes only through a full MS group analysis encompassing motions deemed feasible.

Various levels of calculations have been applied to cluster studies. Each different method has its own advantages and drawbacks. We choose to employ empirical potential energy calculations due to their clear physical insight and relative simplicity. With a coherent set of atomic parameters obtained from thermodynamic data and crystal structures, one can successfully predict most cluster structures and determine the hindering potentials for the nonrigid cluster van der Waals motions. The predictions seem to be quantitative in many cases. At present this is probably the best way to analyze a variety of nonrigid clusters systematically. The approach has, nonetheless, its disadvantages. The major limitation is probably the neglect of interaction directionality, since the potential form is only a function of the interatomic distances. This drawback is most severe for hydrogen-bonding situations. Thus, in spite of all the calculational successes, caution must be exercised with each new structure prediction and/or potential barrier estimation.

We have defined two categories of cluster nonrigidity: (1) local cluster nonrigidity, in which the center of mass of each molecular constituent is fixed, and (2) global cluster nonrigidity, in which at least one of the molecular moieties experiences a center-of-mass displacement from one local potential minimum to another. Internal rotations of solvent molecules belong to category 1. This local nonrigidity is most frequently encountered since hindering potentials are typically small. Category 2 involves multiple cluster configurations of different geometries. This latter nonrigid behavior is difficult to detect experimentally for the following reasons: (1) it is relatively rare compared to local nonrigidity behavior, (2) potential barriers separating local minima are often high enough to prevent nonrigid van der Waals motion, giving rise to different stable isomers, and (3) Franck−Condon factors for transitions involving such large amplitude displacements are likely to be quite small.

Potential barriers for large amplitude rotations and translations tend to increase as the solvent molecules become more complex in terms of interaction potentials (e.g., polar vs nonpolar, hydrogen bonding, etc.). For aromatic solute systems, planar, highly symmetric solute moieties such as benzene or cpd tend to have very low potential barriers for large amplitude van der Waals motions, while substituents on the aromatic ring usually exert extra hindering interactions. Other stronger interactions, (e.g., hydrogen bonding) may even stabilize new cluster configurations.

We have only scratched the surface of nonrigid cluster behavior in this report. Many small molecule clusters have nonrigid behavior as well. Additionally, larger molecule clusters include other aromatic systems (e.g., azabenzene dimers,[89] mixed aromatic dimers, azabenzene/solvent systems[90]) and cyclic ethers and amines.[91] We have only presented a few of the techniques that can be used to determine cluster dynamics and structures. Other methods, such as rotational coherence spectroscopy,[92] can, in principle, be as important as microwave spectroscopy in defining the nature of van der Waals clusters. Dynamic studies of cluster nonrigidity would also be a highly valuable approach to obtaining potential surfaces. Of course, theoretical studies must also become more accurate and of predictive value.

The most important point of this survey of nonrigid cluster behavior is that we need to consider van der Waals clusters from a different point of view and a different theoretical approach than that of the traditional fixed structure/harmonic/small amplitude motion/point group algorithm taken for typical molecules. Application of molecular symmetry group techniques and carefully calculated potential energy surfaces must precede the analysis of spectroscopic data.

Note Added in Proof. We have now studied aniline/NH$_3$ clusters in some detail and, through hole burning spectroscopy, have demonstrated that at least two cluster conformers exist for the aniline(NH$_3$)$_1$ cluster.

A recent paper in *J. Chem. Phys.* (see: Joffe, R. L.; Smith, G. D. A Quantum Chemistry Study of Benzene Dimer. *Gen. Phys. Adv. Abstr.* **1996**, *12* (12), 25 June, 55) suggests that (1) the T-shaped structure is a low-energy saddle point on the conversion path between parallel displaced structures, (2) the planar sandwich structure is a higher-energy interconversion

Feature Article

J. Phys. Chem., Vol. 100, No. 32, 1996 **13365**

saddle point between two parallel displaced structures, and (3) a tilted angle (45°) minimum exists on the path between parallel displaced structure. The authors suggest in their abstract that the large amplitude motion between these structures, through the various saddle points, could explain much of the observed dimer behavior and spectroscopy.

References and Notes

(1) For example: (a) Breen, P. J.; Warren, J. A.; Bernstein, E. R.; Seeman, J. I. *J. Chem. Phys.* **1987**, *87*, 1917. (b) Breen, P. J.; Warren, J. A.; Bernstein, E. R.; Seeman, J. I. *Ibid.* **1987**, *87*, 1927. (c) Breen, P. J.; Warren, J. A.; Bernstein, E. R.; Seeman, J. I. *J. Am. Chem. Soc.* **1987**, *109*, 3453.

(2) (a) Hollas, J. M. *Chem. Soc. Rev.* **1993**, *22*, 371. (b) Ito, M. *J. Phys. Chem.* **1987**, *91*, 517.

(3) See the special issue of: *NATO ASI Ser.*, *Ser. C* **1993**, *410*.

(4) (a) Chakraborty, T.; Lim, E. C. *J. Chem. Phys.* **1993**, *98*, 836. (b) Shin, Y. D.; Saigusa, H.; Zgierski, M. Z.; Zerbetto, F.; Lim, E. C. *J. Chem. Phys.* **1991**, *94*, 3511.

(5) For example: (a) Nowak, R.; Menapace, J. A.; Bernstein, E. R. *J. Chem. Phys.* **1988**, *89*, 1309. (b) Menapace, J. A.; Bernstein, E. R. *J. Phys. Chem.* **1987**, *91*, 2533. (c) Disselkamp, R.; Bernstein, E. R. *J. Chem. Phys.* **1993**, *98*, 4339. (d) Sun, S.; Bernstein, E. R. *J. Chem. Phys.* **1995**, *103*, 4447.

(6) (a) Weber, Th.; Smith, A. M.; Riedle, E.; Neusser, H. J.; Schlag, E. W. *Chem. Phys. Lett.* **1990**, *175*, 79. (b) Hobza, P.; Bludsky, O.; Selzle, H. L.; Schlag, E. W. *J. Chem. Phys.* **1993**, *98*, 6223. (c) Ohshima, Y.; Kohguchi, H.; Endo, Y. *Chem. Phys. Lett.* **1991**, *184*, 21.

(7) (a) Bunker, P. R. *Vibrational Spectra and Structure*; Durig, J. R., Ed.; Dekker: New York, 1975; Vol. 3, Chapter 1. (b) Papousek, D.; Stone, J. M. R.; Spirko, V. *J. Mol. Spectrosc.* **1973**, *48*, 17 and references therein.

(8) (a) Nesbitt, D. J. *Chem. Rev.* **1988**, *88*, 843. (b) Nesbitt, D. J. *Faraday Discuss.* **1994**, *97*, 1. (c) Fraser, G. T. *Int. Rev. Phys. Chem.* **1991**, *10*, 189. (d) Cohen, R. C.; Saykally, R. J. *J. Chem. Phys.* **1992**, *96*, 1024 and references therein.

(9) For example: Bernstein, E. R.; Law, K.; Schauer, M. *J. Chem. Phys.* **1984**, *80*, 634.

(10) For example: Engdahl, A.; Nelander, B. *J. Phys. Chem.* **1985**, *89*, 2860.

(11) For example: (a) Gryff-Keller, A. *Wiad. Chem.* **1989**, *43*, 799. (b) Szymanski, S. *Ibid.* **1989**, *43*, 767.

(12) (a) Balle, T. J.; Flygare, W. H. *Rev. Sci. Instrum.* **1981**, *52*, 33. (b) Chuang, C.; Hawley, C. J.; Emilsson, T.; Gutowsky, H. S. *Ibid.* **1990**, *61*, 1629.

(13) (a) Gutowsky, H. S.; Emilsson, T.; Arunan, E. *J. Chem. Phys.* **1993**, *99*, 4883. (b) Suzuki, S.; Green, P. G.; Bumgarner, R. E.; Dasgupta, S.; Goddard, W. A., III; Blake, G. A. *Science* **1992**, *157*, 942.

(14) (a) Blake, G. A.; Laughlin, K. B.; Cohen, R. C.; Busarow, K. L.; Gwo, D.-H.; Schmuttenmaer, C. A.; Steyert, D. W.; Saykally, R. J. *Rev. Sci. Instrum.* **1991**, *62*, 1693. (b) Blake, G. A.; Laughlin, K. B.; Cohen, R. C.; Busarow, K. L.; Gwo, D.-H.; Schmuttenmaer, C. A.; Steyert, D. W.; Saykally, R. J. *Ibid.* **1991**, *62*, 1701. (c) Farhoomand, J.; Blake, G. A.; Ferking, M. A.; Pickett, H. M. *J. Appl. Phys.* **1985**, *57*, 1763. (d) Busarow, K. L.; Blake, G. A.; Laughlin, K. B.; Cohen, R. C.; Lee, Y. T.; Saykally, R. J. *J. Chem. Phys.* **1988**, *89*, 1268.

(15) (a) Ebata, T.; Furukawa, M.; Suzuki, T.; Ito, M. *J. Opt Soc. Am.* **1990**, *7*, 1890. (b) Frye, D.; Lapierre, L.; Dai, H.-L. *Ibid.* **1990**, *7*, 1905. (c) Takayanagi, M.; Hanazaki, I. *Ibid.* **1990**, *7*, 1898. (d) Dai, H.-L.; Field, R. W. *Molecular Dynamics and Spectroscopy by Stimulated Emission Pumping*; World Scientific: Singapore, 1995.

(16) (a) Felker, P. M.; Maxton, P. M.; Schaeffer, M. W. *Chem. Rev.* **1994**, *94*, 1787. (b) Hartland, G. V.; Henson, B. F.; Venturo, V. A.; Hertz, R. A.; Felker, P. M. *J. Opt. Soc. Am.* **1990**, *7*, 1950. (c) See ref 15d, Chapter 8, p 279.

(17) (a) Pribble, R. N.; Zwier, T. S. *Science* **1994**, *265*, 75. (b) Pribble, R. N.; Zwier, T. S. *Faraday Discuss.* **1994**, *97*, 229.

(18) (a) Venturo, V. A.; Felker, P. M. *J. Chem. Phys.* **1993**, *99*, 748. (b) Venturo, V. A.; Felker, P. M. *J. Phys. Chem.* **1993**, *97*, 4882. (c) Henson, B. F.; Hartland, G. V.; Venturo, V. A.; Hertz, R. A.; Felker, P. M. *Chem. Phys. Lett.* **1991**, *176*, 91. (d) Ebata, T.; Hamakado, M.; Moriyama, S.; Morioka, Y.; Ito, M. *Chem. Phys. Lett.* **1992**, *199*, 33.

(19) Page, R. H.; Shen, Y. R.; Lee, Y. T. *J. Chem. Phys.* **1988**, *88*, 4621.

(20) See: (a) reference 17. (b) Pribble, R. N.; Garrett, A. W.; Haber, K.; Zwier, T. S. *J. Chem. Phys.* **1995**, *103*, 531.

(21) See: (a) reference 6a. (b) Weber, Th.; von Bargen, A.; Riedle, E.; Neusser, H. J. *J. Chem. Phys.* **1990**, *92*, 90.

(22) (a) Lipert, R. J.; Colson, S. D. *Chem. Phys. Lett.* **1989**, *161*, 303. (b) Lipert, R. J.; Colson, S. D. *J. Phys. Chem.* **1989**, *93*, 3894.

(23) For example: (a) Saigusa, H.; Sun, S.; Lim, E. C. *J. Chem. Phys.* **1992**, *97*, 9072. (b) Chakraborty, T.; Sun, S.; Lim, E. C. *J. Am. Chem. Soc.*

(24) *1994*, *116*, 10050. (c) Wittmeyer, S. A.; Topp, M. R. *Chem. Phys. Lett.* **1989**, *163*, 261.

(24) Buckingham, A. D.; Fowler, P. W.; Hutson, J. M. *Chem. Rev.* **1988**, *88*, 963.

(25) Hobza, P.; Zahradník, R. *Chem. Rev.* **1988**, *88*, 871.

(26) Boys, S. F.; Bernardi, F. *Mol. Phys.* **1970**, *19*, 553.

(27) Hobza, P.; Selzle, H. L.; Schlag, E. W. *Chem. Rev.* **1994**, *94*, 1767.

(28) For example: McGuire, R. F.; Momany, F. A.; Scheraga, H. A. *J. Phys. Chem.* **1972**, *76*, 375.

(29) Karasawa, N.; Dasgupta, S.; Goddard, W. A. *J. Phys. Chem.* **1991**, *95*, 2260.

(30) (a) Momany, F. A.; Carruthers, L. M.; McGuire, R. F.; Scheraga, H. A. *J. Phys. Chem.* **1974**, *78*, 1595. (b) Nemethy, G.; Pottle, M. S.; Scheraga, H. A. *J. Phys. Chem.* **1983**, *87*, 1883.

(31) Wilson, E. B., Jr.; Decius, J. C.; Cross, P. C. *Molecular Vibrations, Theory of Infrared and Raman Vibrational Spectra*; McGraw-Hill: New York, 1955.

(32) (a) Bernstein, E. R. *J. Chem. Phys.* **1970**, *52*, 4701. (b) Li, S.; Bernstein, E. R. *J. Chem. Phys.* **1991**, *95*, 1577.

(33) Kung, C. Y.; Miller, T. A.; Kennedy, R. A. *Philos. Trans. R. Soc. London* **1988**, *A324*, 233.

(34) See: (a) Reference 7a. (b) Bunker, P. R. *Molecular Symmetry and Spectroscopy*; Academic: New York, 1979; Chapter 12. (c) Hougen, J. T. *J. Chem. Phys.* **1963**, *39*, 358. (d) Altman, S. L. *Induced Representations in Crystals and Molecules*; Academic: New York, 1977. (e) Longuett-Higgins, H. C. *Mol. Phys.* **1963**, *6*, 445.

(35) Menapace, J. A.; Bernstein, E. R. *J. Phys. Chem.* **1987**, *91*, 2843.

(36) (a) Longuet-Higgins, H. C. *Mol. Phys.* **1963**, *6*, 445. (b) Hougen, J. T. *J. Chem. Phys.* **1962**, *37*, 1433.

(37) Brupbacher, Th.; Bauder, A. *J. Chem. Phys.* **1993**, *99*, 9394.

(38) Nagy, P. I.; Ulmer II, C. W.; Smith, D. A. *J. Chem. Phys.* **1995**, *102*, 6812.

(39) Larin, A. V.; Poljanskii, S. V.; Trubnikov, D. N. *Chem. Phys. Lett.* **1993**, *213*, 619.

(40) Maxton, P. M.; Schaeffer, M. W.; Ohline, S. M.; Kim, W.; Venturo, V. A.; Felker, P. M. *J. Chem. Phys.* **1994**, *101*, 8391.

(41) Wanna, J.; Menapace, J. A.; Bernstein, E. R. *J. Chem. Phys.* **1986**, *85*, 1795.

(42) Gotch, A. J.; Garrett, A. W.; Severance, D. L.; Zwier, T. S. *Chem. Phys. Lett.* **1991**, *178*, 121.

(43) (a) Gotch, A. J.; Zwier, T. S. *J. Chem. Phys.* **1992**, *96*, 3388. (b) Garrett, A. W.; Zwier, T. S. *Ibid.* **1992**, *96*, 3402.

(44) Börnsen, K. O.; Selzle, H. L.; Schlag, E. W. *Z. Naturforsch.* **1990**, *45A*, 1217.

(45) Maxton, P. M.; Schaeffer, M. W.; Felker, P. M. *Chem. Phys. Lett.* **1995**, *241*, 603.

(46) Karlström, G.; Linse, P.; Wallqvist, A.; Jönsson, B. *J. Am. Chem. Soc.* **1983**, *105*, 3777.

(47) (a) Cheney, B. V.; Schulz, M. W.; Cheney, J.; Richards, W. G. *J. Am. Chem. Soc.* **1988**, *110*, 4195. (b) Cheney, B. V.; Schulz, M. W. *J. Phys. Chem.* **1990**, *94*, 6268.

(48) Brédas, J. L.; Street, G. B. *J. Chem. Phys.* **1989**, *90*, 7291.

(49) (a) Linse, P. *J. Comput. Chem.* **1988**, *9*, 505. (b) Linse, P. *J. Am. Chem. Soc.* **1990**, *112*, 1744.

(50) (a) Augspurger, J. D.; Dykstra, C. E.; Zwier, T. S. *J. Phys. Chem.* **1992**, *96*, 7252. (b) Augspurger, J. D.; Dykstra, C. E.; Zwier, T. S. *Ibid.* **1993**, *97*, 980.

(51) Schauer, M.; Bernstein, E. R. *J. Chem. Phys.* **1985**, *82*, 726.

(52) Sakaki, S.; Kato, K.; Miyazaki, T.; Musashi, Y.; Ohkubo, K.; Ihara, H.; Hirayama, C. *J. Chem. Soc., Faraday Trans.* **1993**, *89*, 659.

(53) Bernstein, E. R.; Colson, S. D.; Kopelove, R.; Robinson, G. W. *J. Chem. Phys.* **1968**, *48*, 5596.

(54) (a) Janda, K. C.; Hemminger, J. C.; Win, J. S.; Novick, S. E.; Harris, S. J.; Klemperer, W. *J. Chem. Phys* **1975**, *63*, 1419. (b) Steed, J. M.; Dixon, T. A.; Klemperer, W. *J. Chem. Phys* **1979**, *70*, 4940.

(55) Hopkins, J. B.; Powers, D. E.; Smalley, R. E. *J. Phys. Chem.* **1981**, *85*, 3739.

(56) Langridge-Smith, P. R. R.; Brumbaugh, D. V.; Haynam, C. A.; Levy, D. H. *J. Phys. Chem.* **1981**, *85*, 3742.

(57) Shinohara, H.; Nishi, N. *J. Chem. Phys.* **1989**, *91*, 6743.

(58) Law, K. S.; Schauer, M.; Bernstein, E. R. *J. Chem. Phys.* **1984**, *81*, 4871.

(59) Börnsen, K. O.; Selzle, H. L.; Schlag, E. W. *J. Chem. Phys.* **1986**, *85*, 1726.

(60) Schauer, M.; Bernstein, E. R. *J. Chem Phys* **1985**, *82*, 3722.

(61) (a) Fung, K. H.; Selzle, H. L.; Schlag, E. W. *J. Phys. Chem.* **1983**, *87*, 5113. (b) Schlag, E. W.; Selzle, H. L. *J. Chem. Soc., Faraday Trans.* **1990**, *86*, 1.

(62) Scherzer, W.; Krätzschmar, O.; Selzle, H. L.; Schlag, E. W. *Z. Naturforsch.* **1992**, *47A*, 1248.

(63) Arunan, E.; Gutowsky, H. S. *J. Chem. Phys.* **1993**, *98*, 4294.

(64) Henson, B. F.; Hartland, G. V.; Venturo, V. A.; Felker, P. M. *J. Chem. Phys.* **1989**, *91*, 2751.

(65) Henson, B. F.; Hartland, G. V.; Venturo, V. A.; Felker, P. M. *J. Chem. Phys.* **1989**, *91*, 2189.

(66) Williams, D. E. *Acta Crystallogr.* **1980**, *A36*, 715.

(67) Van der Waal, B. W. *Chem. Phys. Lett.* **1986**, *123*, 69.

(68) (a) Fraga, S. *J. Comput. Chem.* **1982**, *3*, 329. (b) Fraga, S. *Comput. Phys. Commun.* **1983**, *29*, 351.

(69) (a) Torrens, F.; Sánchez-Marín, J.; Ortí, E.; Nebot-Gil, I. *J. Chem. Soc., Perkin Trans.* **1987**, *2*, 943. (b) Rubio, M.; Torrens, F.; Sánchez-Marín, J. *J. Comput. Chem.* **1993**, *14*, 647.

(70) Hobza, P.; Selzle, H. L.; Schlag, E. W. *J. Chem. Phys.* **1990**, *93*, 5893.

(71) Hobza, P.; Selzle, H. L.; Schlag, E. W. *J. Phys. Chem.* **1993**, *97*, 3937.

(72) Hobza, P.; Selzle, H. L.; Schlag, E. W. *J. Am. Chem. Soc.* **1994**, *116*, 3500.

(73) Kiermeier, A.; Ernstberger, B.; Neusser, H. J.; Schlag, E. W. *J. Phys. Chem.* **1988**, *92*, 3785.

(74) Shoemaker, R. L.; Flygare, W. H. *J. Chem. Phys.* **1969**, *51*, 2988.

(75) Vrbancich, J.; Ritchie, G. L. D. *J. Chem. Soc., Faraday Trans. 2* **1980**, *76*, 648.

(76) Hirshfelder, J. O.; Curtis, C. F.; Bird, R. B. *Molecular Theory of Gases and Liquids*; Wiley: New York, 1954.

(77) (a) Momany, F. A.; McGuire, R. F.; Burgess, A. W.; Scheraga, H. A. *J. Phys. Chem.* **1975**, *79*, 2361. (b) Momany, F. A.; Carruthers, L. M.; Scheraga, H. A. *Ibid.* **1974**, *78*, 1621. (c) Scott, R. A.; Scheraga, H. A. *J. Chem. Phys.* **1966**, *45*, 2091 and references therein.

(78) Schauer, M.; Law, K. S.; Bernstein, E. R. *J. Chem. Phys.* **1984**, *81*, 49.

(79) Schauer, M.; Law, K. S.; Bernstein, E. R. *J. Chem. Phys.* **1985**, *82*, 736.

(80) Li, S.; Bernstein, E. R. *J. Chem. Phys.* **1992**, *97*, 792.

(81) Li, S.; Bernstein, E. R. *J. Chem. Phys.* **1992**, *97*, 804.

(82) (a) Nimlos, M. R.; Young, M. A.; Bernstein, E. R.; Kelley, D. F. *J. Chem. Phys.* **1989**, *91*, 5268. (b) Hineman, M. F.; Kim, S. K.; Bernstein, E. R.; Kelley, D. F. *J. Chem. Phys.* **1992**, *96*, 4904.

(83) Coutant, B.; Brechignac, P. *J. Chem. Phys.* **1989**, *91*, 1978.

(84) Lister, D. G.; Tyler, J. K. *Chem. Commun.* **1966**, 152.

(85) Bernstein, E. R. *J. Phys. Chem.* **1992**, *96*, 10105.

(86) Im, H. S.; Bernstein, E. R. *J. Chem. Phys.* **1991**, *95*, 6326.

(87) Disselkamp, R.; Bernstein, E. R. *J. Phys. Chem.* **1994**, *98*, 7260.

(88) Bray, J. A.; Taylor, D. P.; Yao, J.; Bernstein, E. R. Unpublished work on picolyl and lutidyl radicals and CX_2: species.

(89) For example: (a) Wanna, J.; Menapace, J. A.; Bernstein, E. R. *J. Chem. Phys.* **1986**, *85*, 777. (b) Wanna, J.; Bernstein, E. R. *Ibid.* **1986**, *85*, 3243.

(90) For example: (a) Wanna, J.; Bernstein, E. R. *J. Chem. Phys.* **1987**, *86*, 6707. (b) Kim, S. K.; Bernstein, E. R. *J. Phys. Chem.* **1990**, *94*, 3531.

(91) Shang, Q. Y.; Bernstein, E. R. *Chem. Rev.* **1994**, *94*, 2015.

(92) (a) Felker, P. M.; Zewail, A. H. *J. Chem. Phys.* **1987**, *86*, 2460. (b) Baskin, J. S.; Felker, P. M.; Zewail, A. H. *Ibid.* **1987**, *86*, 2483. (c) Felker, P. M. *J. Phys. Chem.* **1992**, *96*, 7844. (d) Topp, M. R. *J. Chem. Phys.* **1995**, *92*, 310 and references therein.